The Abdus Salam
International Centre for Theoretical Physics

United Nations
Educational, Scientific and
Cultural Organization

IAEA
International Atomic Energy Agency

2137-26

Joint ICTP-IAEA Advanced Workshop on Multi-Scale Modelling for Characterization and Basic Understanding of Radiation Damage Mechanisms in Materials

12 - 23 April 2010

Atomistic simulation of a swift ion track development in a model Ni-Al alloy

N. Lazarev

Akhiezer Institute for Theoretical Physics
Kharkov
Ukraine

Atomistic simulation of a swift ion track development in a model Ni-Al alloy

Nikolai Lazarev

Kharkov Institute of Physics and Technology, Ukraine

n.lazarev@kipt.kharkov.ua

Collaboration:

Christian Abromeit

Helmholtz-Zentrum Berlin für Materialien und Energie

Rolf Gotthardt

École Polytechnique Fédérale de Lausanne

Robin Schäublin

EPFL SB CRPP Groupe Matériaux, PSI

Outline

- Basic concepts of track formation
- MT and shape memory alloys
- Hysteretic behavior at reversible MT
- Kinetics of transformation
- Stress-controlled MT
- MT in ordered Ni_5Al_3 and Ni_7Al_5 alloys
- Grain Boundary Effect
- Phase transformations at track development

Nuclear and electronic stopping power

$$\frac{dE}{dx}^{(total)} = \frac{dE}{dx}^{(nucl)} + \frac{dE}{dx}^{(electr)}$$

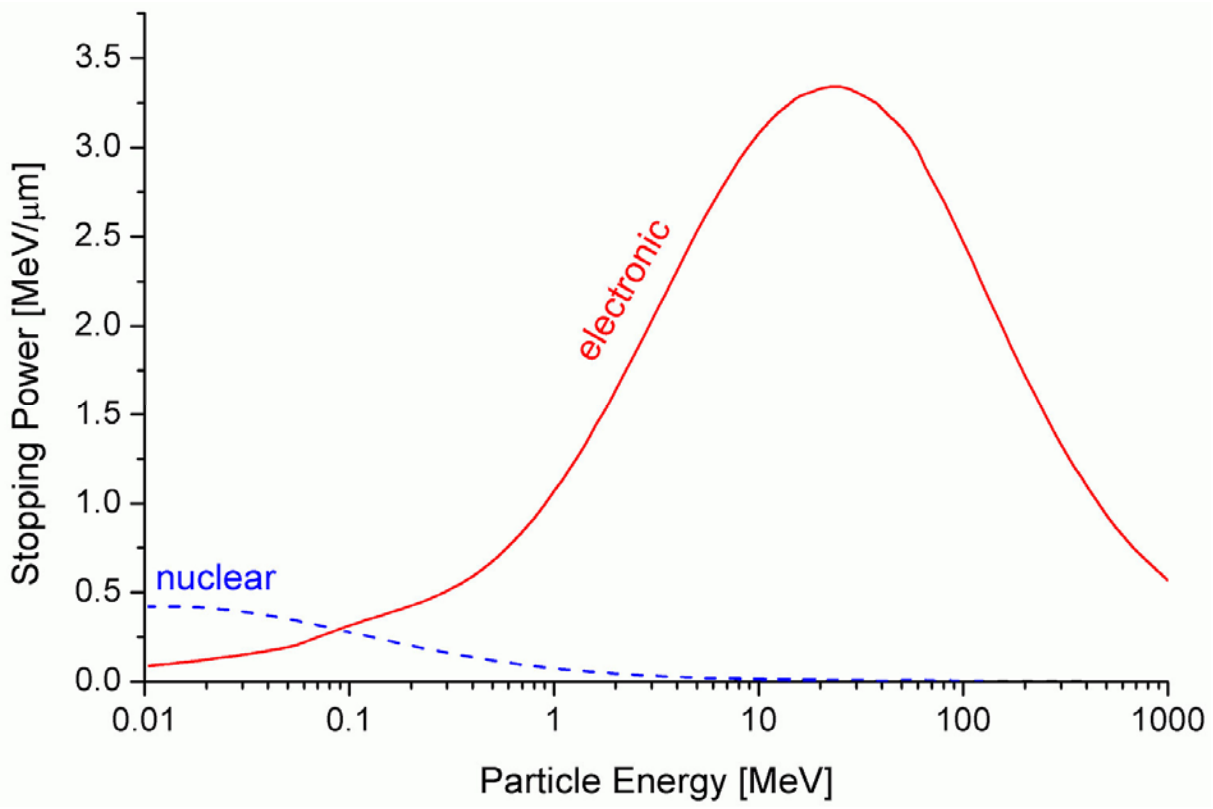

Stopping power for Al ions in Al. The nuclear stopping curve typically reaches maximum at energies of ~1 keV/nucleon, the electronic one ~1MeV/ nucleon.

Track formation by swift heavy ion

E_i ~ 0.1-10 GeV

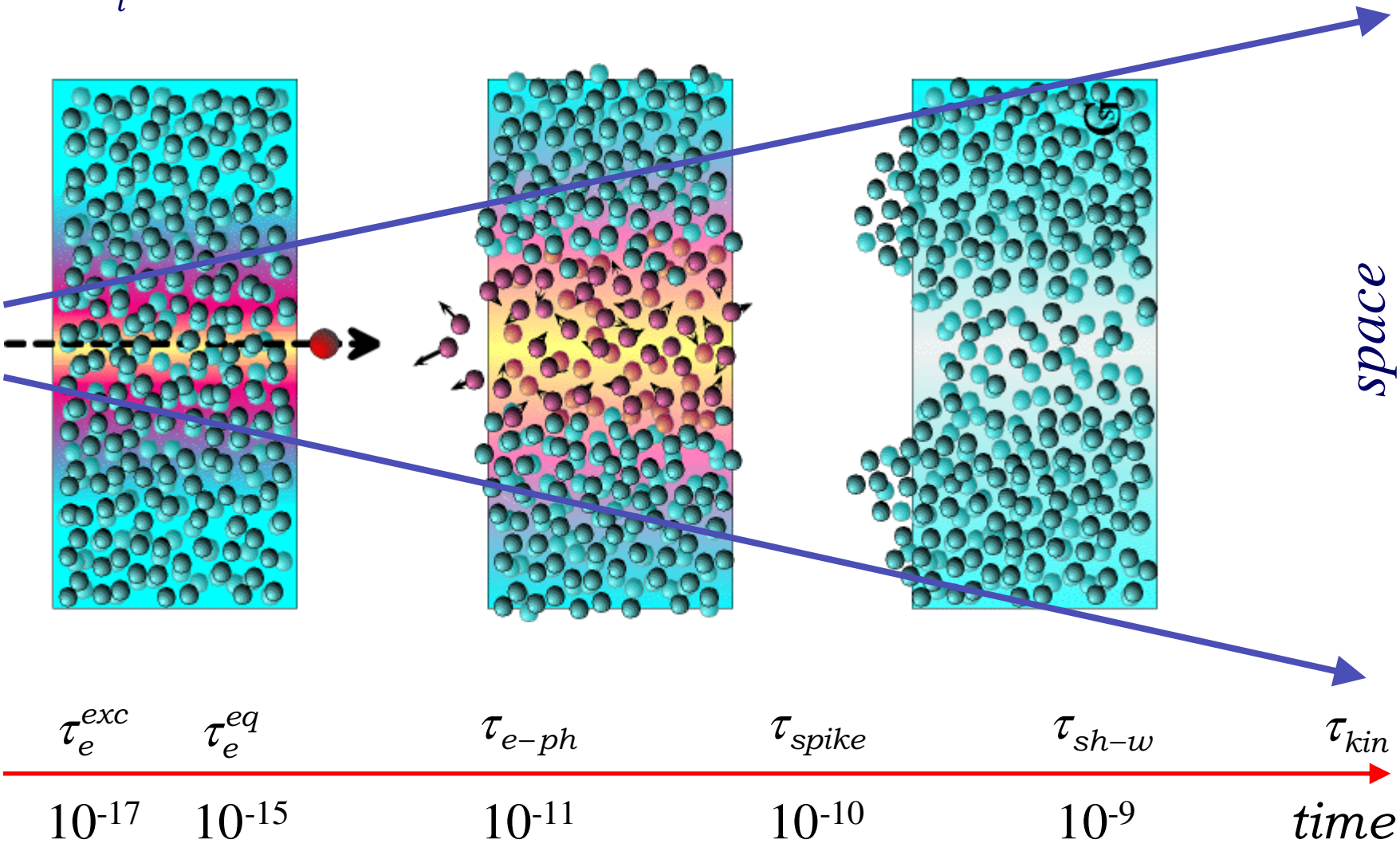

Thermal spike model: analytical description

M.I. Kaganov, I.M. Lifshits, L.V. Tanatarov, Sov. Phys. JETP 4 (1957) 175

$$C_e(T_e)\frac{\partial T_e}{\partial t} = \frac{1}{r}\frac{\partial}{\partial r} rK_e(T_e)\frac{\partial}{\partial r}T_e - g(T_e - T_a) + B(r,t)$$

$$C_a(T_a)\frac{\partial T_a}{\partial t} = \frac{1}{r}\frac{\partial}{\partial r} rK_a(T_a)\frac{\partial}{\partial r}T_a - g(T_a - T_c)$$

$$\frac{dE}{dx} = \iint B(r,t)\,dr\,dt$$

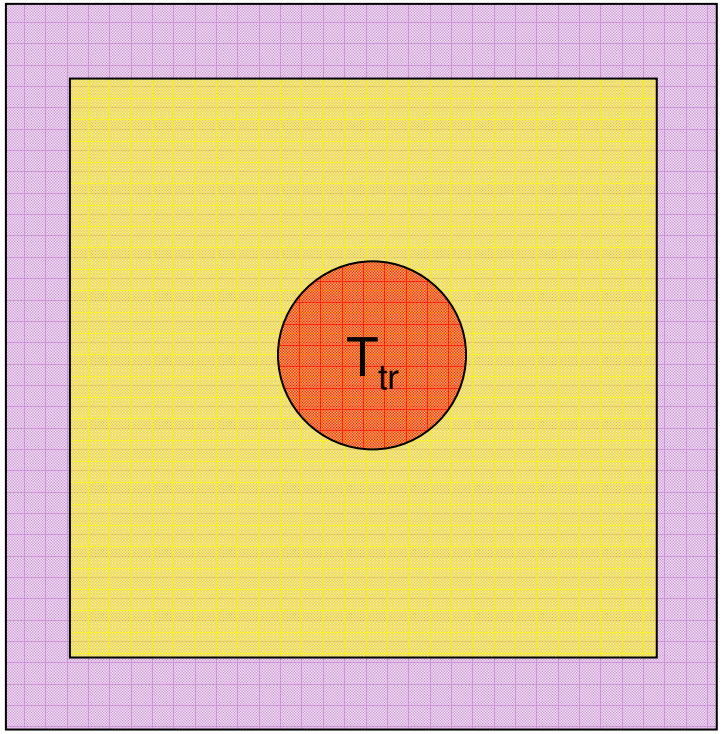

Experimental study of electronic temperatures in heavy ion tracks

M. Caron, H. Rothard, M. Toulemonde, B. Gervais, M. Beuve, NIMPR B245 (2006) 36–40

Values of the electron–phonon coupling g (in 10^{10} $Wcm^{-3}K^{-1}$) for different metals assuming $n_e/n_a = 1$ [25]

Metals ($W/cm^3/K$)	Kaganov et al. [26] ($W/cm^3/K$)	Swift heavy ions ($W/cm^3/K$)	Calculated threshold (keV/nm)	From experimen (keV/nm)
Cu	13×10^{10}			
Au	2.3×10^{10}			
Fe	119×10^{10}	144×10^{10} [16]	~45	~40 [30]
a-$Fe_{85}B_{15}$	2400×10^{10}	500×10^{10} [34,35]	~15	~13 [31]
Bi	20×10^{10}	13×10^{10} [33]	~30	~30 [25]
Ti	203×10^{10}	1000×10^{10} [16]	~12	~7 [32]
Graphite	2700×10^{10}	3000×10^{10}	~8	~7 [33]
Co	90×10^{10}	345×10^{10} [16]	~32	~35 [32]
Zr	85×10^{10}	260×10^{10} [16]	~29	~30 [32]

Swift ion track observations in the NiTi

A. Barbu, A. Dunlop, A. Hardouin Duparc, G. Jaskierowicz, N. Lorenzelli, NIMPR B145 (1998) 354.

Ion	E (GeV)	T	Fluence (cm^{-2})	$dE/dx\|_e$ (keV/nm)	Velocity (m/s)	Structure	Figures	Comments and mean track diameters D_m (nm)
Kr	0.71	85 K	5×10^{10}	17	4.0×10^{7}	M–M		No visible damage
			5×10^{11}					
Xe	0.82	85 K	1.3×10^{11}	32	3.5×10^{7}	M–M		No visible damage
		85 K	1.0×10^{12}			M–M		No visible damage
		85 K	2.6×10^{13}			M–M	17	Monoclinic → B2 (X ray)
Ta	0.98	85 K	5×10^{10}	46	3.2×10^{7}	A–M	1c	$D_m = 4.2$
Pb	0.84	85 K	5×10^{10}	52	2.8×10^{7}	A–M	1b, 4c	$D_m = 5.7$
		85 K	5×10^{10}			M–M	5, 6, 7	$D_m = 12.8$
		85 K	1.8×10^{13}			M–M	13, 14	(am + B2)
		85 K	7.2×10^{13}			M–M	15	Totally am
Pb	0.84	300 K	5×10^{10}	52	2.8×10^{7}	A + M	9	Tracks only in M
			10^{12}			M	11, 12	Tracks (am + B2)
			10^{13}			A	16	No tracks but cascades
U	0.76	85 K	5×10^{10}	57	2.5×10^{7}	A–M	1a, 2, 4b, 10	$D_m = 13.1$
		85 K	5×10^{10}			M–M	8	$D_m = 17.5$
		85 K	5×10^{11}			A–M	3	$D_m = 13.1$
U	4.6	10 K	5×10^{10}	52	6.1×10^{7}	A–M	4a	$D_m = 6.5$

MD simulation of sputtering from a cylindrical track

O.J. Tucker, D.S. Ivanov, L.V. Zhigilei, R.E. Johnson, E.M. Bringa, NIMPR B 228 (2005) 163

Snapshots from simulations of thermal spike in Au.

$dE/dx = N_{exc}E_{exc}/d \sim m\pi R^2_{cyl}E_{exc}$

$R_{cyl} = 10$ Å, $E_{exc} = 10$ eV, $t = 4$ ps

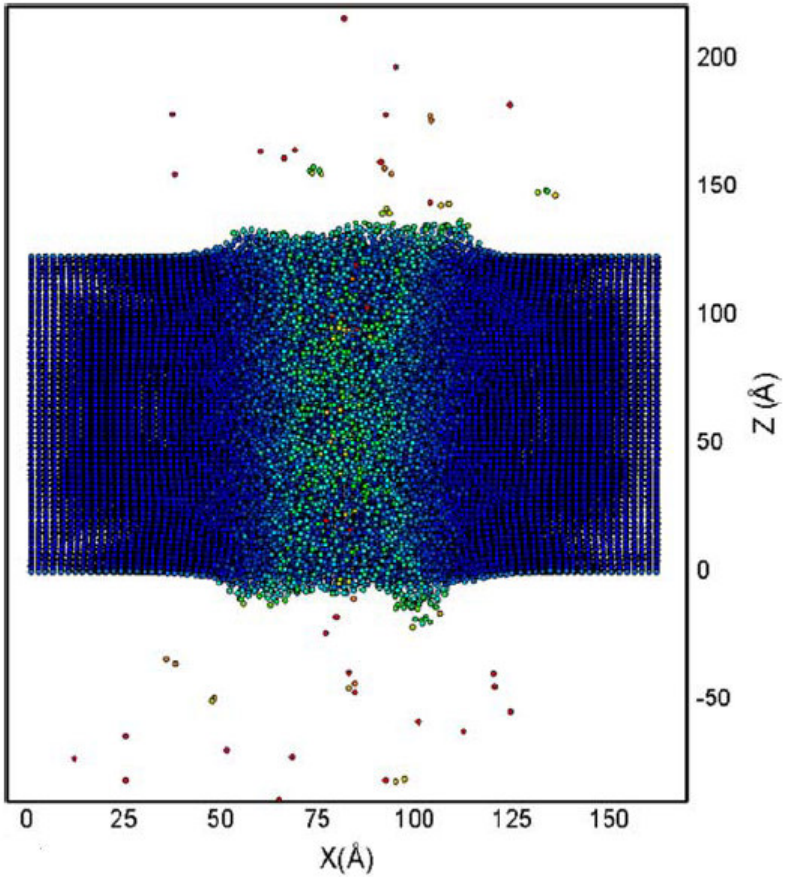

Microstructure of the 350 MeV Au ion irradiated Ti-Ni thin film

T. LaGrange, R. Schäublin, D. S. Grummon, C. Abromeit, R. Gotthardt, *Phil. Mag.* ***85*** *(2005) 577*

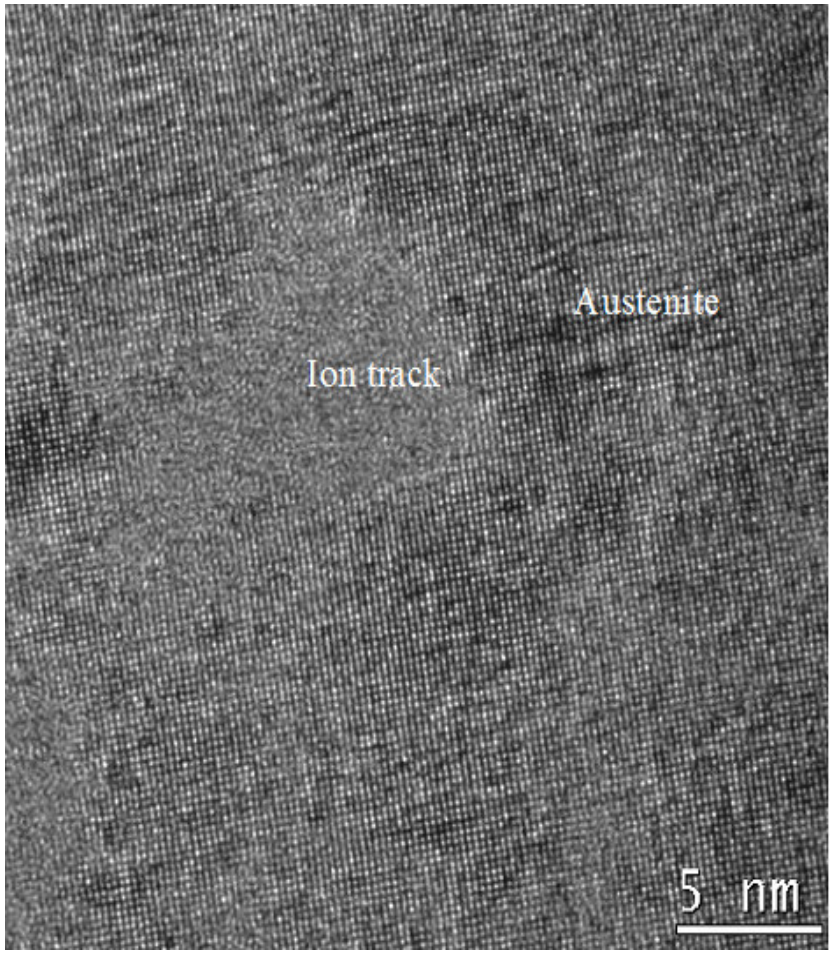

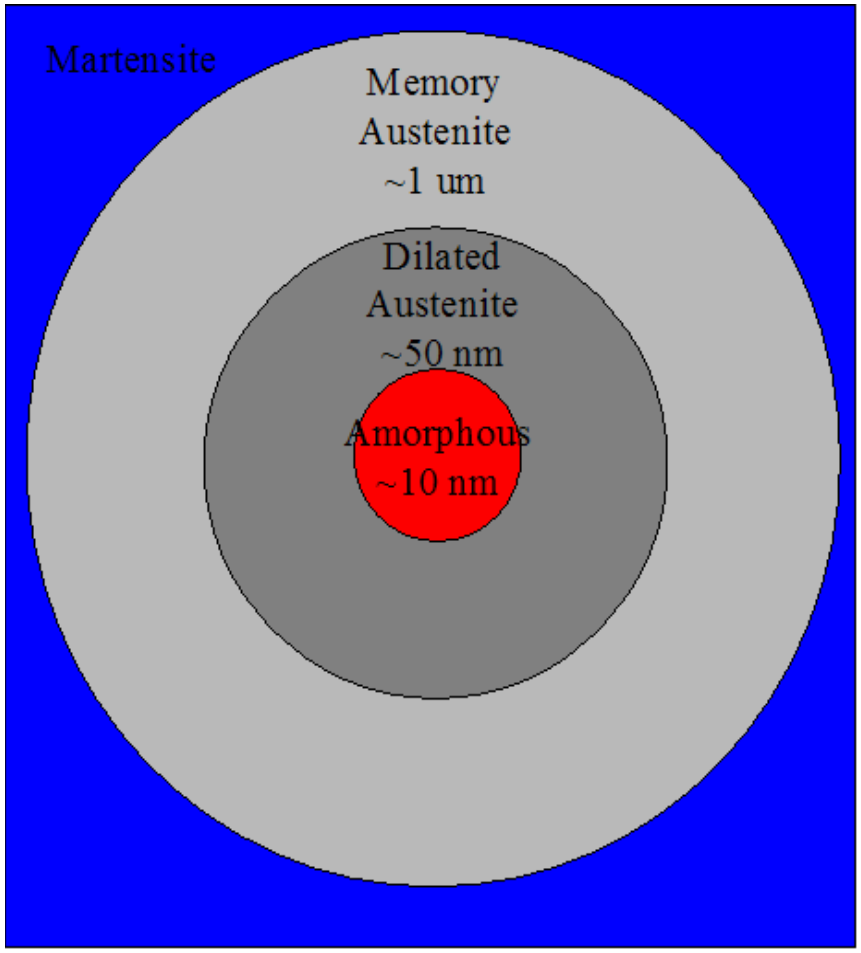

Problems

MT at fast heating/cooling

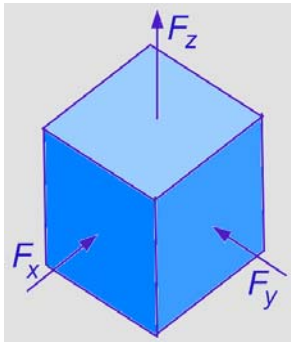

Stress-controlled MT

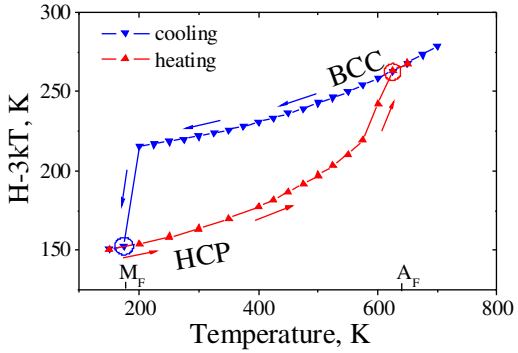

Effect of interfaces

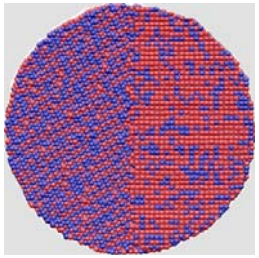

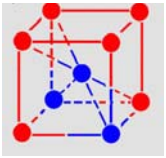

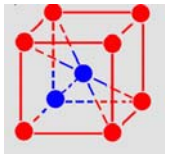

Compositional order-disorder

Local structure order

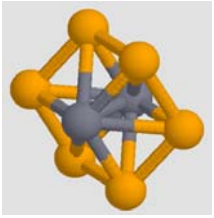

Lattice correspondence: austenite - martensite lattices

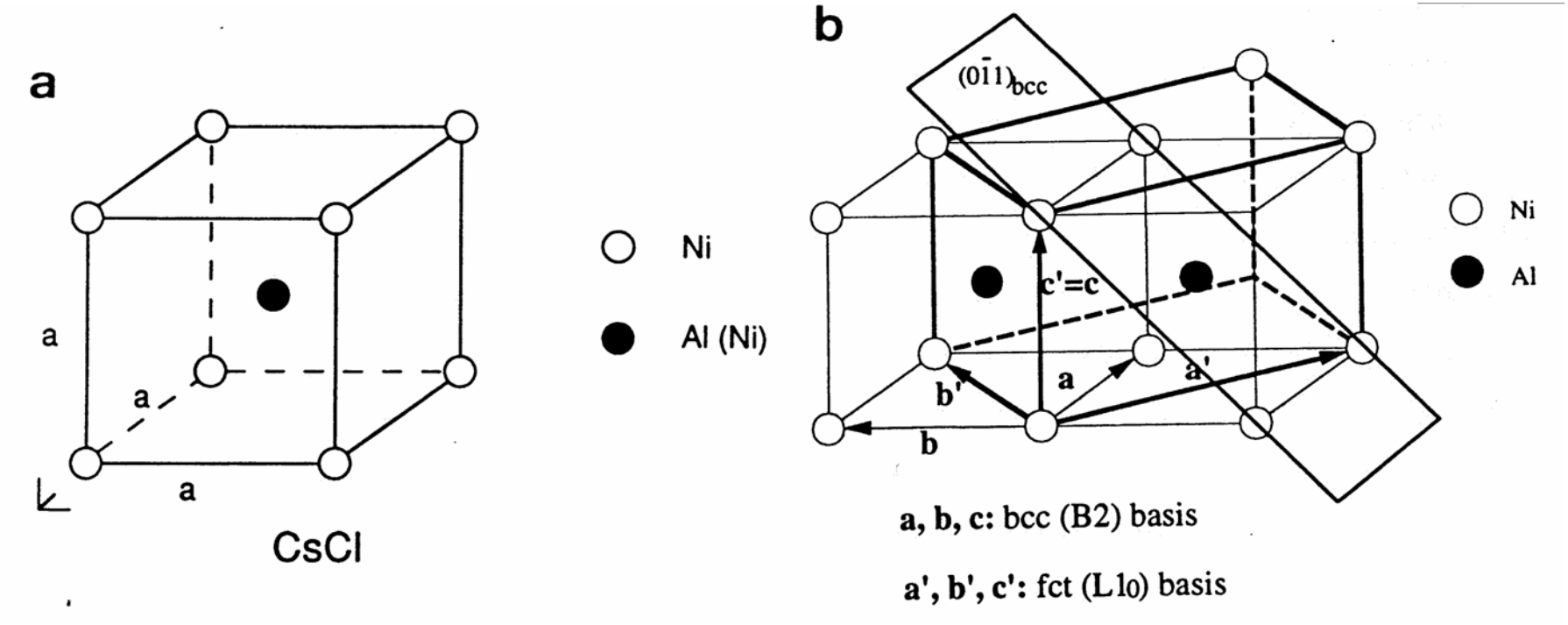

austenite B2 structure (CsCl ordering)

martensite $L1_0$ lattices

Shape Memory Alloys

Ni-Ti, Cu-Zn-Al, Cu-Al-Ni, *Au-Cd, Fe-Pt, Ni-Al*

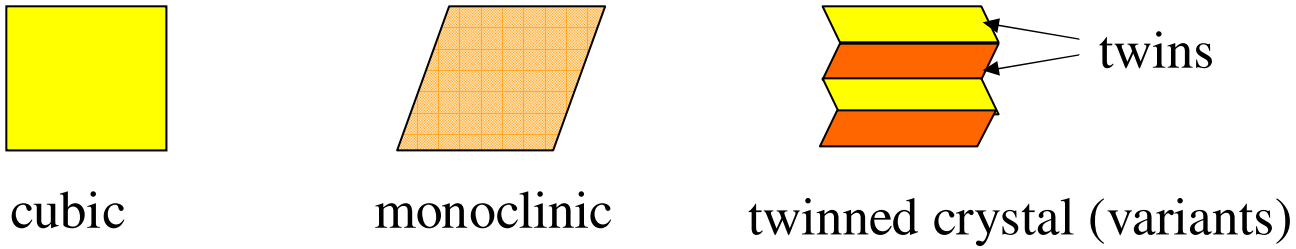

A non-diffusion transformation which can be induced by:

a) temperature change

b) applying stress

Phase diagram of Ni-Al system

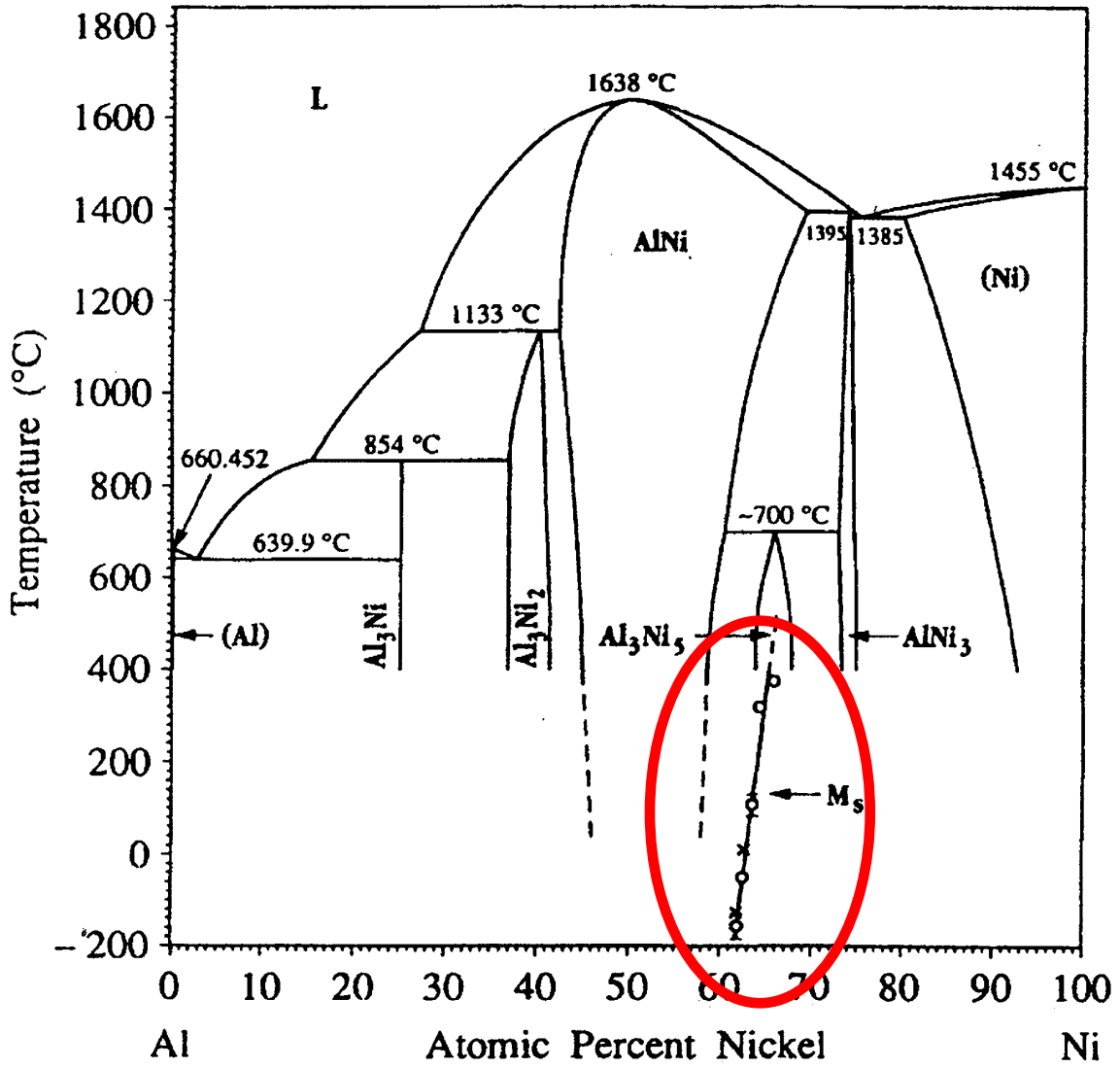

H. Okamoto,
J. Phase Equilibria
14(2) (1993) 257

Simulation Setup

$$Ni_xAl_{100-x}, \quad x = 60 \div 70$$

Molecular Dynamics with Empirical force-field

EAM potential: $$U = \sum_{ij} V(r_{ij}) + \sum_{i} F(\overline{\rho}_i)$$

Limitations:

System size $N = 10^4 \div 10^7$

Time window $t = 1 \div 20\ ns$

Potentials

A.F. Voter and S.P. Chen, *Accurate Interatomic Potentials for Ni, Al, and Ni3Al*, Mat. Res. Soc. Symp. Proc. 82 (1987) 175.

D. Farkas, B. Mutasa, C. Vailhe, K. Ternes, *Interatomic potentials for B2 NiAl and martensitic phases.* Modeling Simul. Mater. Sci. Eng. 3 (1995) 201-214.

M. Yan, V. Vitek and S. P. Chen, *Many-body central force potentials and properties of grain boundaries in NiAl*, Acta Mater. 44 (1996) 4351-4365.

Y. Mishin, M. J. Mehl and D. A. Papaconstantopoulos, *Embedded-atom potential for B2-NiAl*, Phys. Rev. B65 (2002) 224114.

N. I. Papanicolaou, H. Chamatia, G. A. Evangelakisa, D. A. Papaconstantopoulos, *Second-moment interatomic potential for Al, Ni and Ni–Al alloys, and molecular dynamics application*, Comp. Mater. Sc. 27 (2003) 191-198.

Song Yua, Chong-Yu Wanga, Tao Yua, Jun Cai, *Self-diffusion in the intermetallic compounds NiAl and Ni3Al: An embedded atom method study*, Physica B 396 (2007) 138–144.

Temperature-controlled MT at constant external stress

N. P. Lazarev, C. Abromeit, R. Schäublin and R. Gotthardt, Solid-Solid Phase Transformations in Inorganic Materials, TMS publications, 2005, Vol. 2, p. 715.

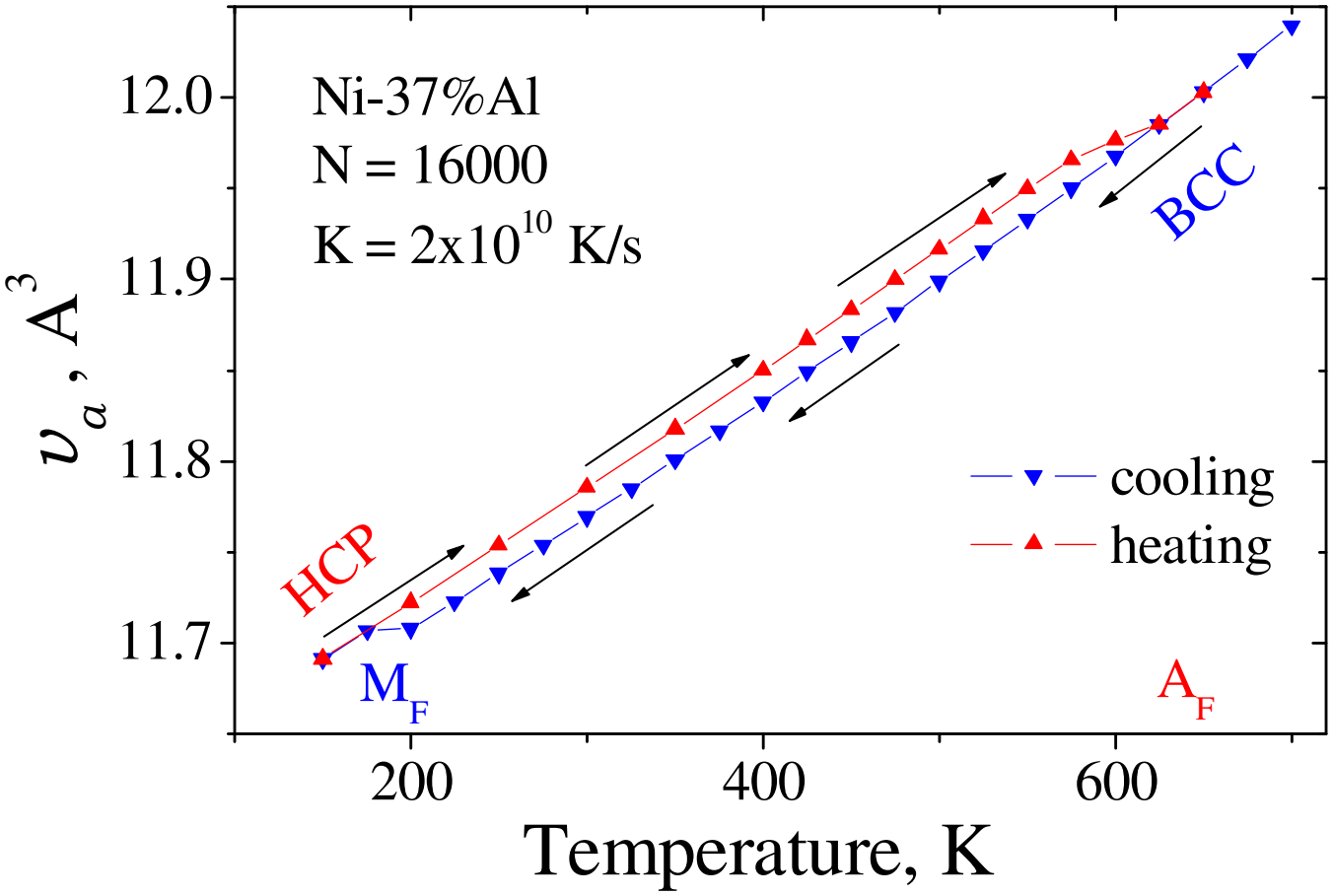

- *Reversible phase transformation*

Shape Changes of Simulated Box

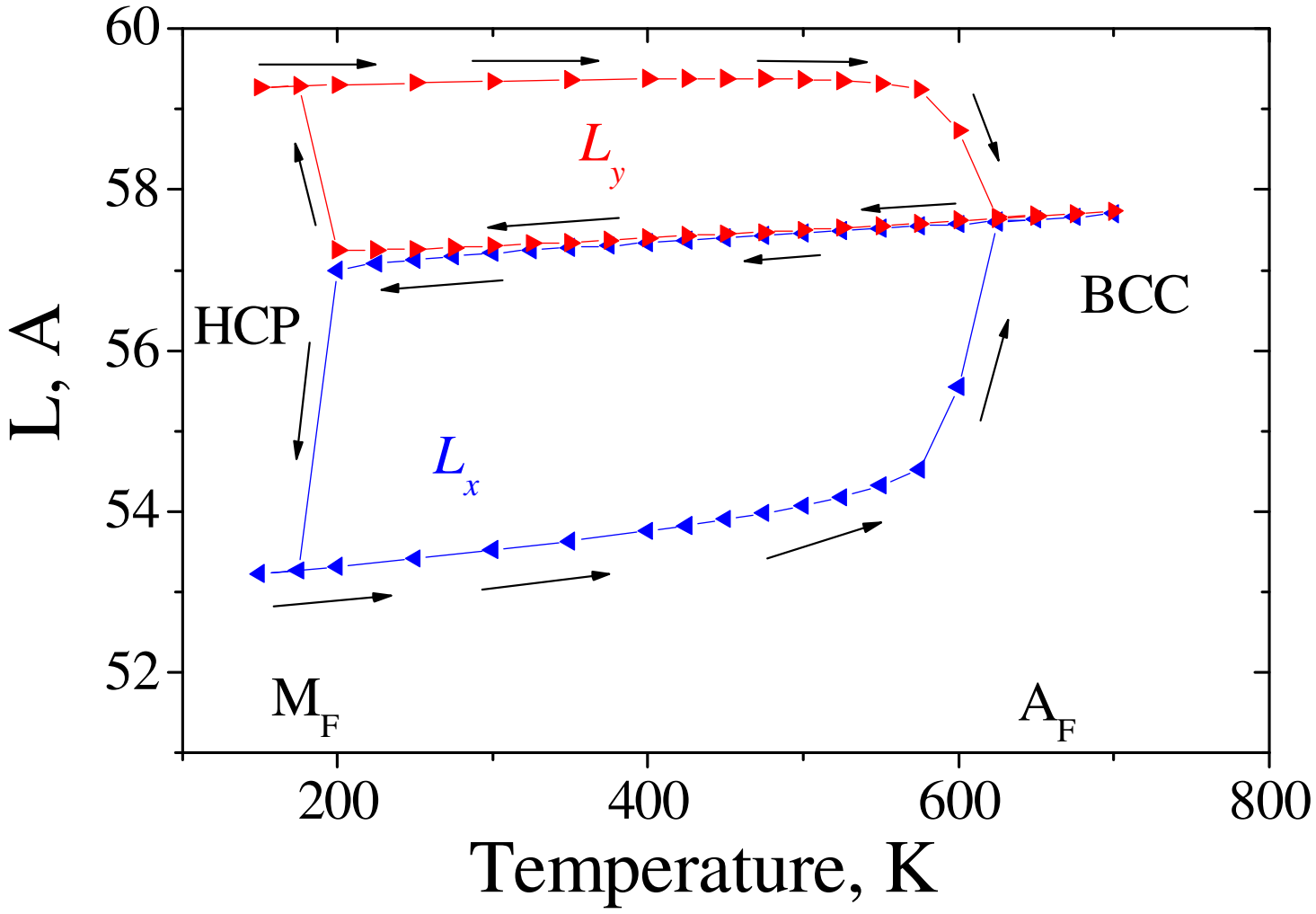

- *Linear dimensions are more sensitive to MPT than average volume*

Enthalpy at Reversible MTs

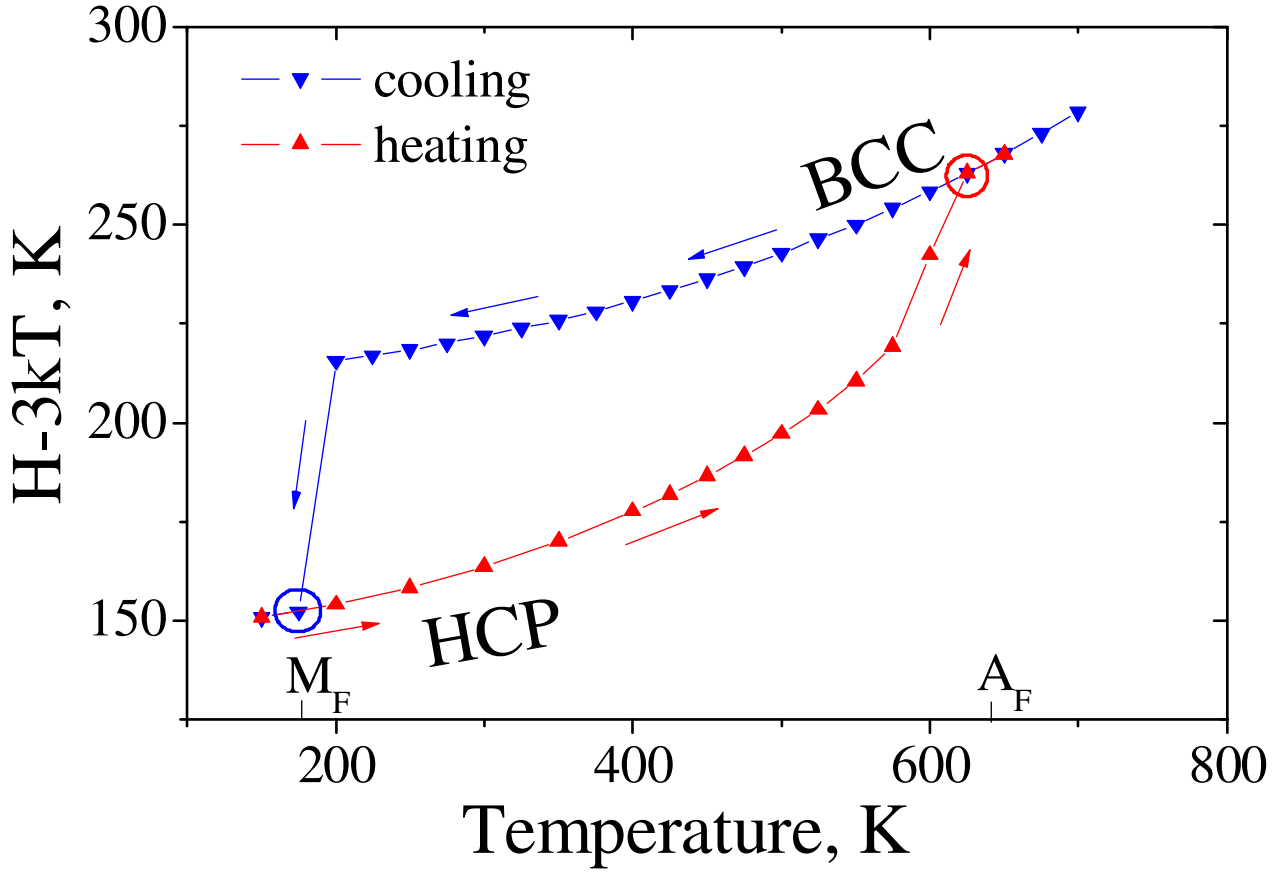

- *The 1-st order phase transformations: A→M →A*

Hysteretic behavior of different samples at equal composition Ni-37%Al.

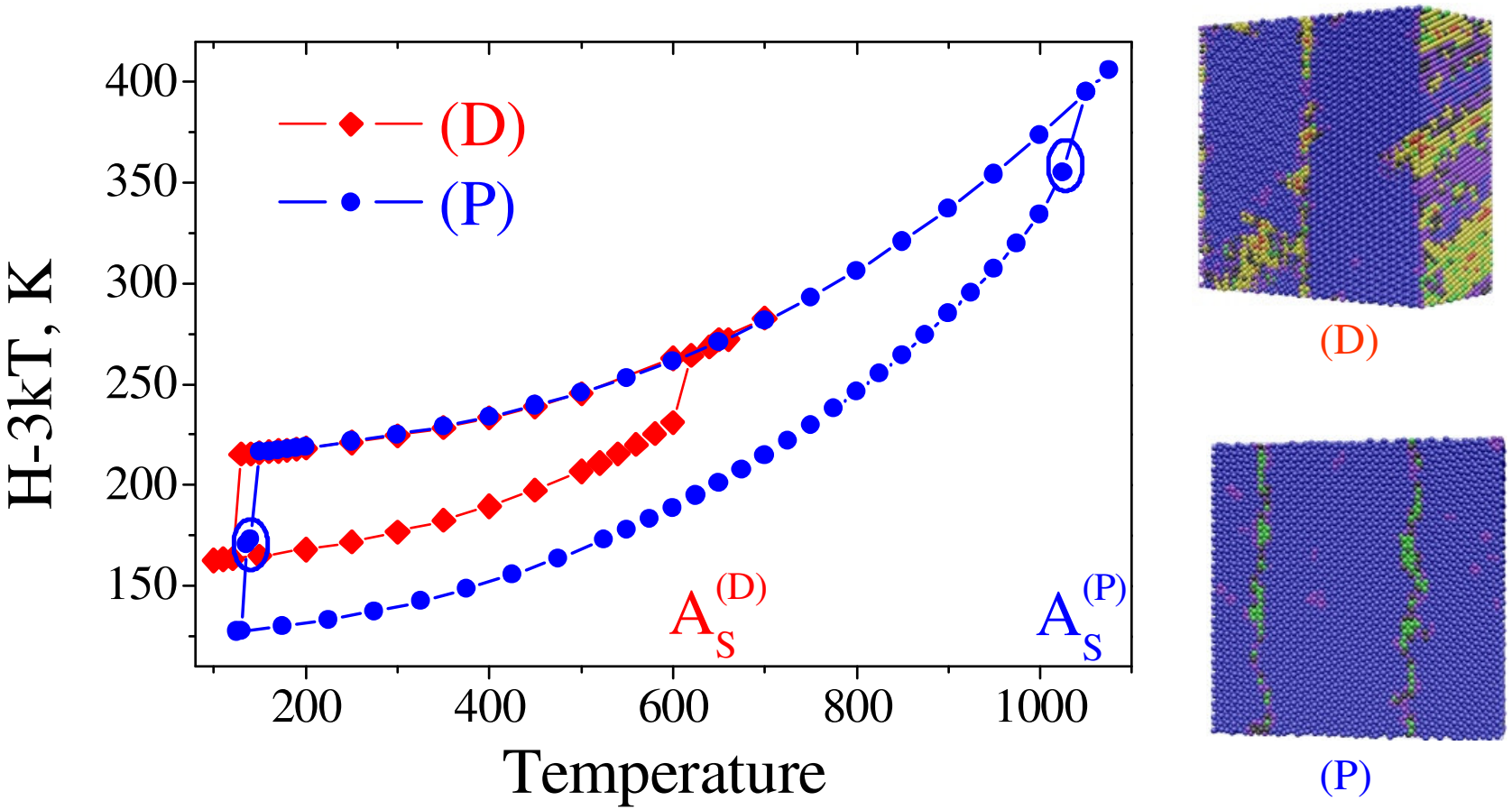

- *Hysteresis width essentially depends on defect structure of martensite state*

Atomic displacements during cycle A →M →A

N. P. Lazarev, C. Abromeit, R. Schäublin, R. Gotthardt, J. Appl. Phys. 100 (2006) 063520

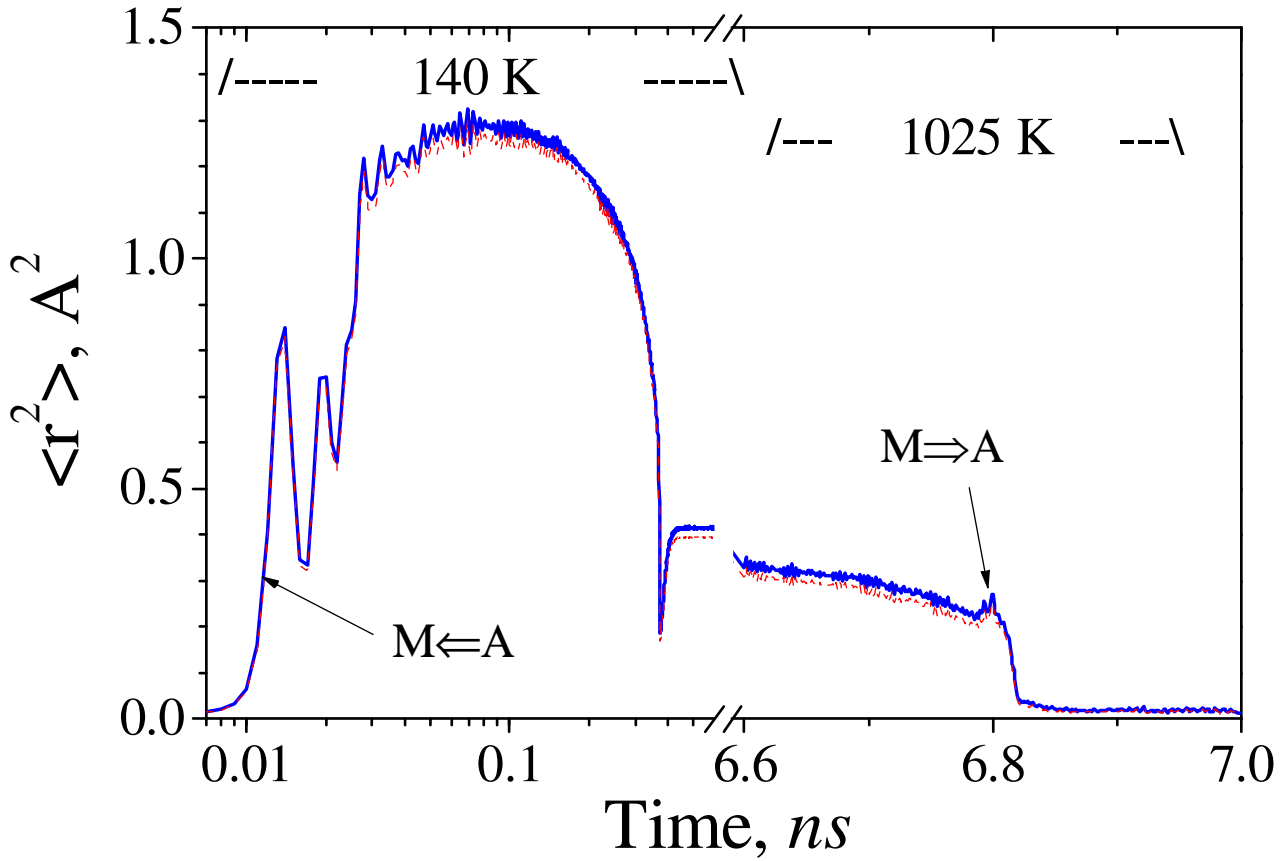

- *Non-diffusional transformations and completely reversible*

Composition dependent MPT

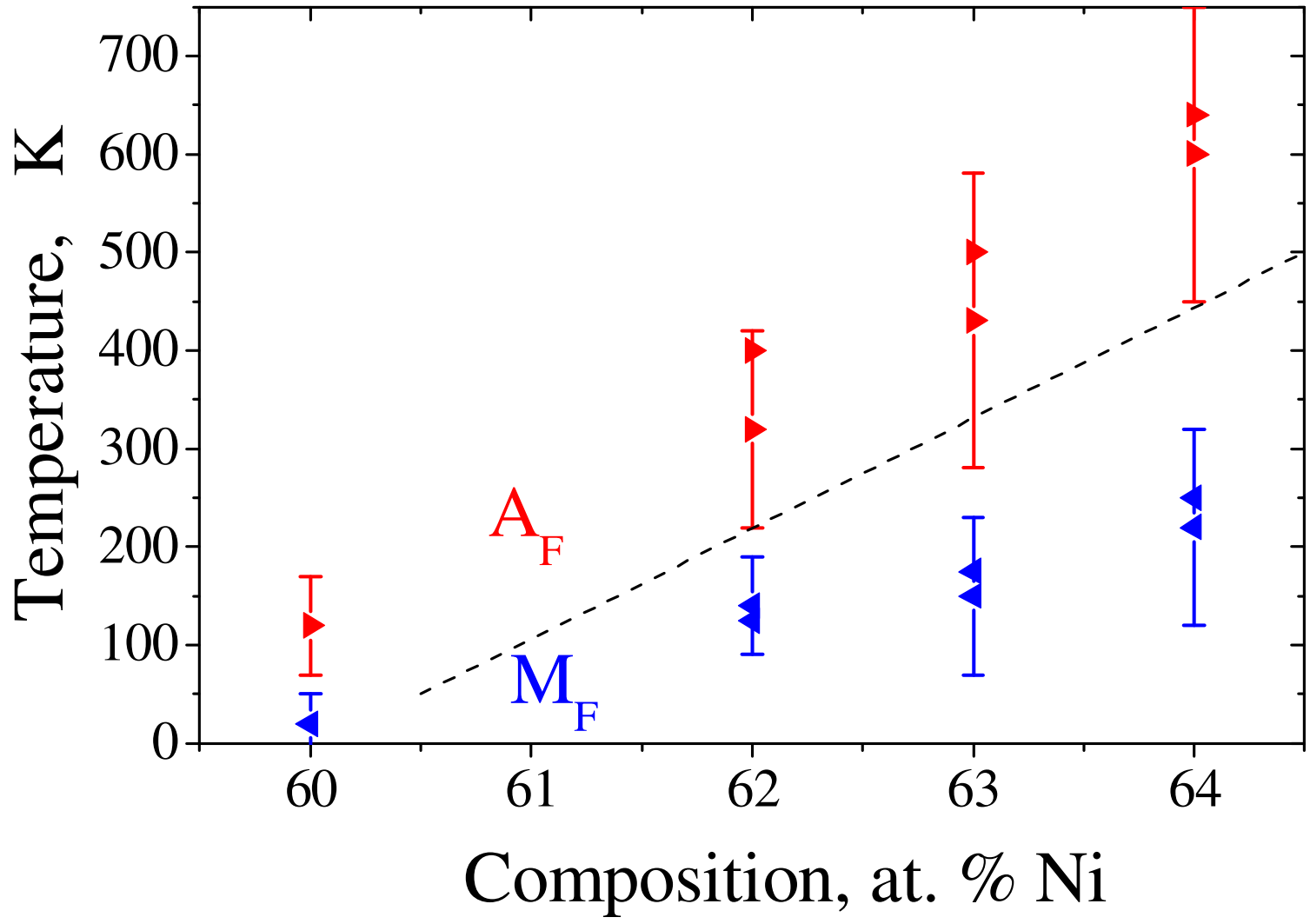

- *MPT is observed in narrow composition interval: 60-65 at. % Ni*

Cylinder under pressure, $Ni_{60}Al_{40}$

Perfect FCC + HCP
Distorted FCC + HCP
Perfect BCC
Distorted BCC
Perf. & Dist. ICO
Gas atoms
Unclassified

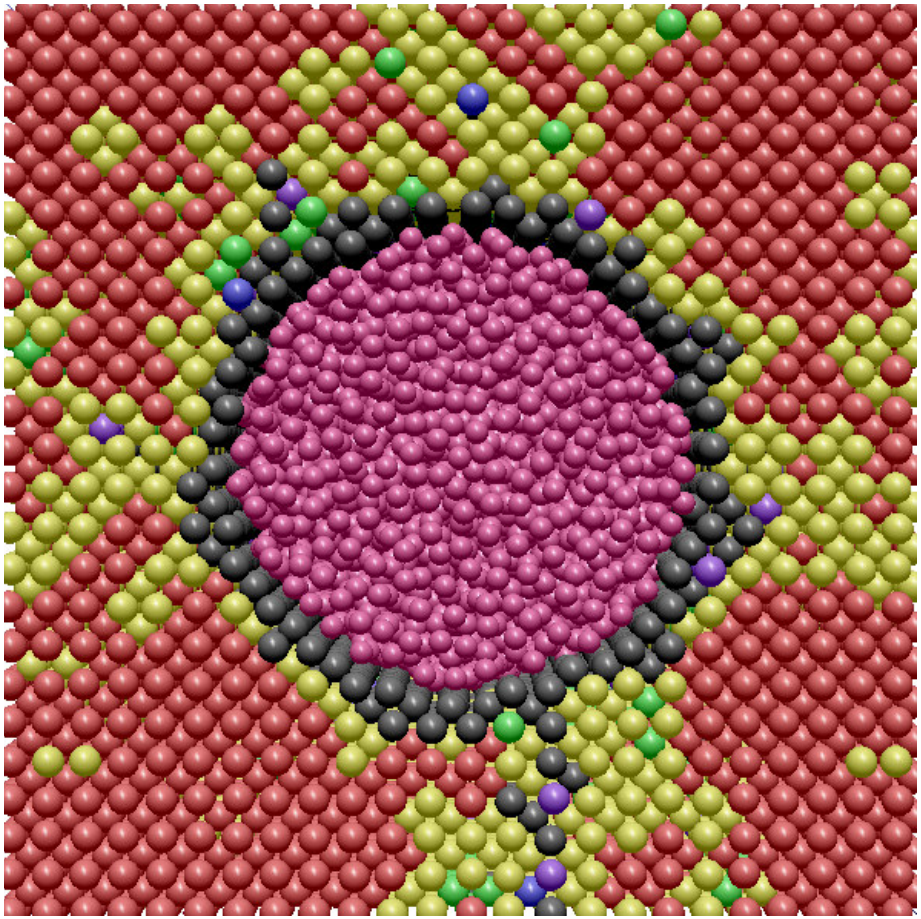

Cylinder under pressure, $Ni_{60}Al_{40}$

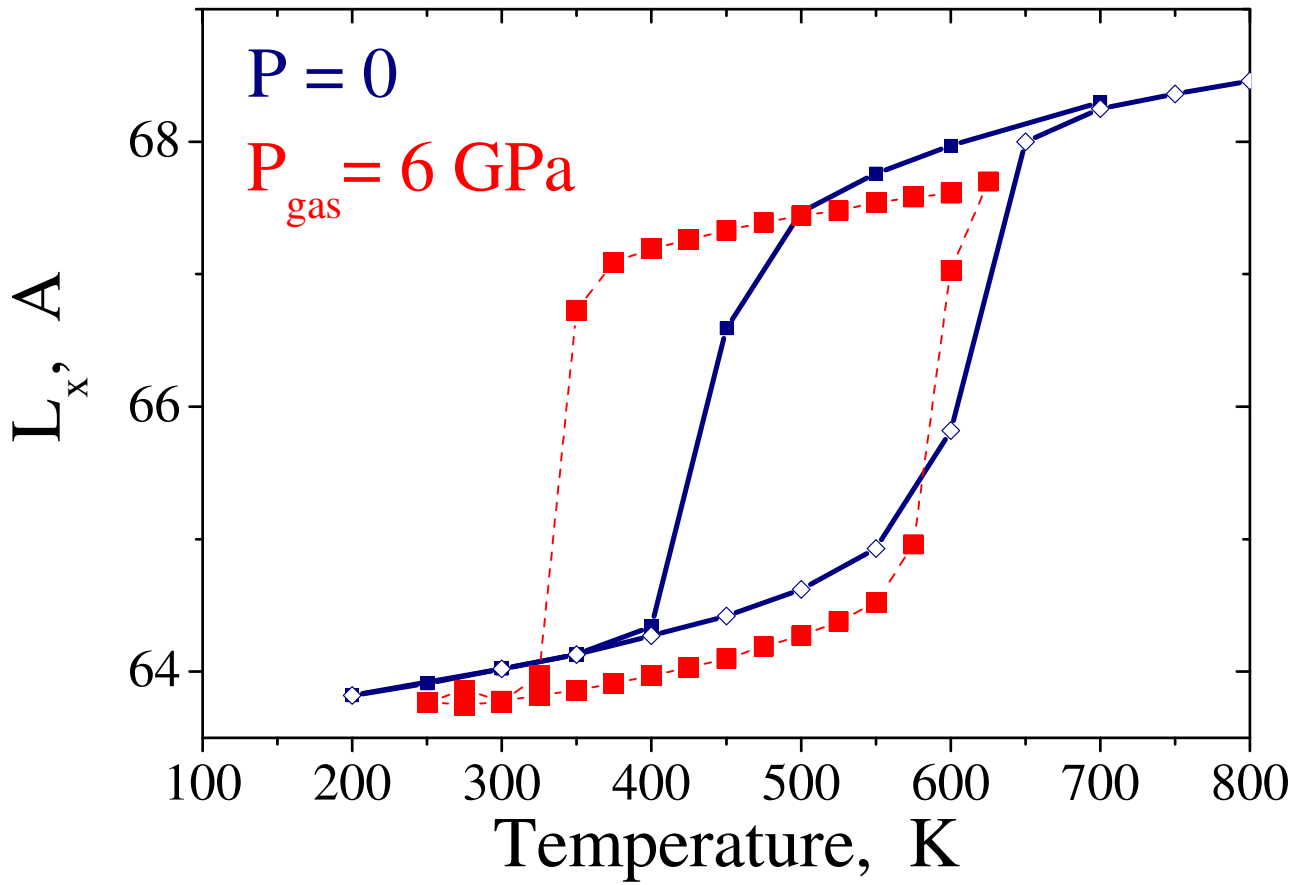

Stress-Controlled MPTs at Constant Temperature

Multi-axial compression/tension

$$\sigma_{xx} = \sigma_{yy} = -\sigma_{zz}/2$$

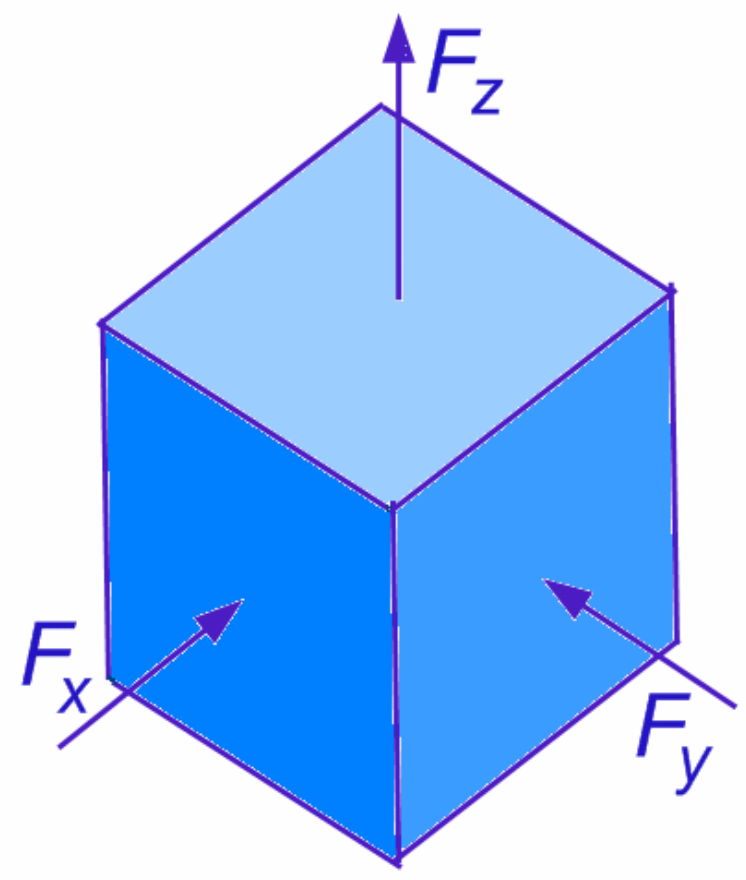

Stress dependence

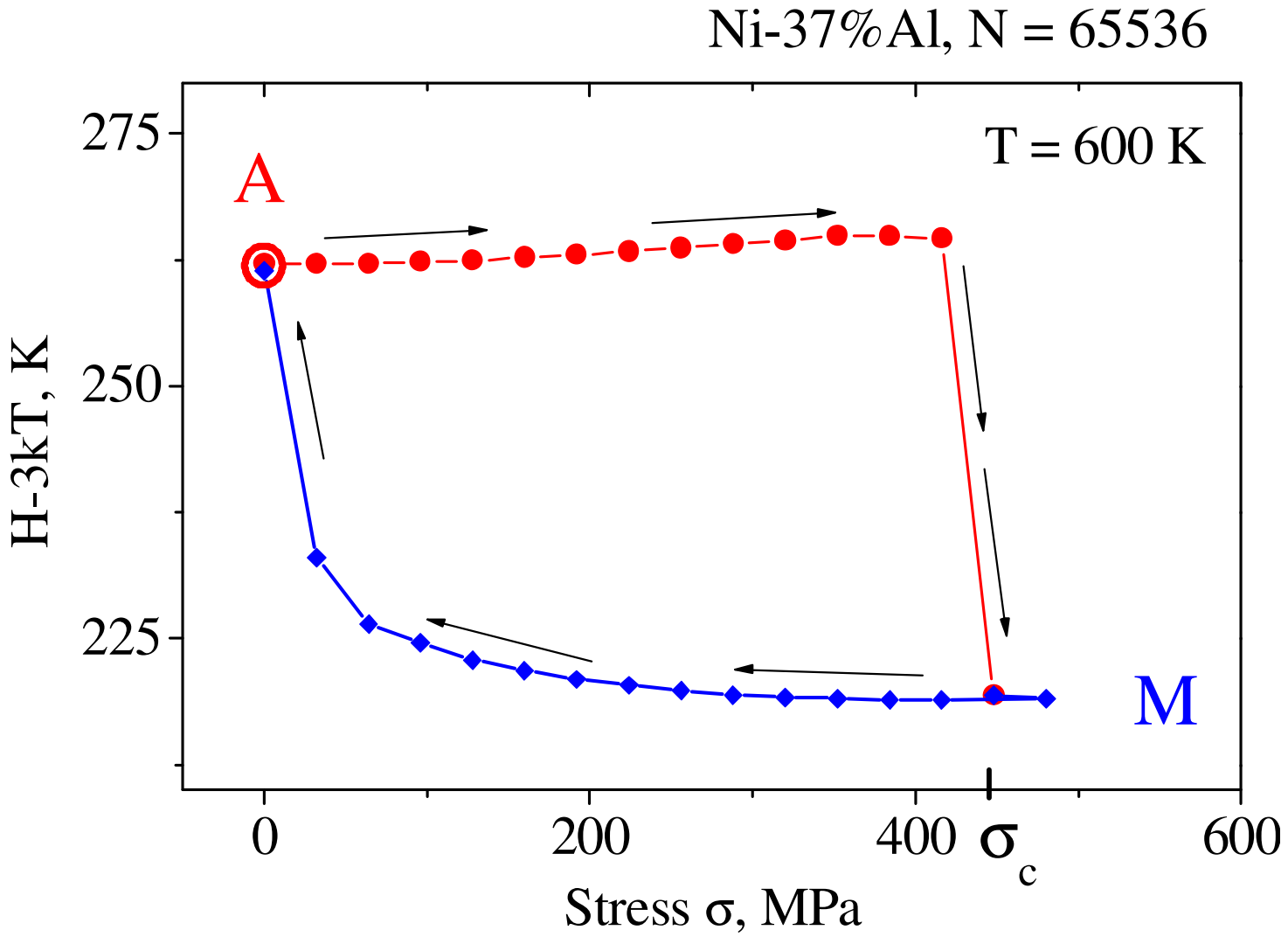

- *Reversibility on Stress*

Map of M_F-States

N. P. Lazarev, C. Abromeit, R. Schäublin, R. Gotthardt, Materials Science and Engineering A481–482 (2008) 205

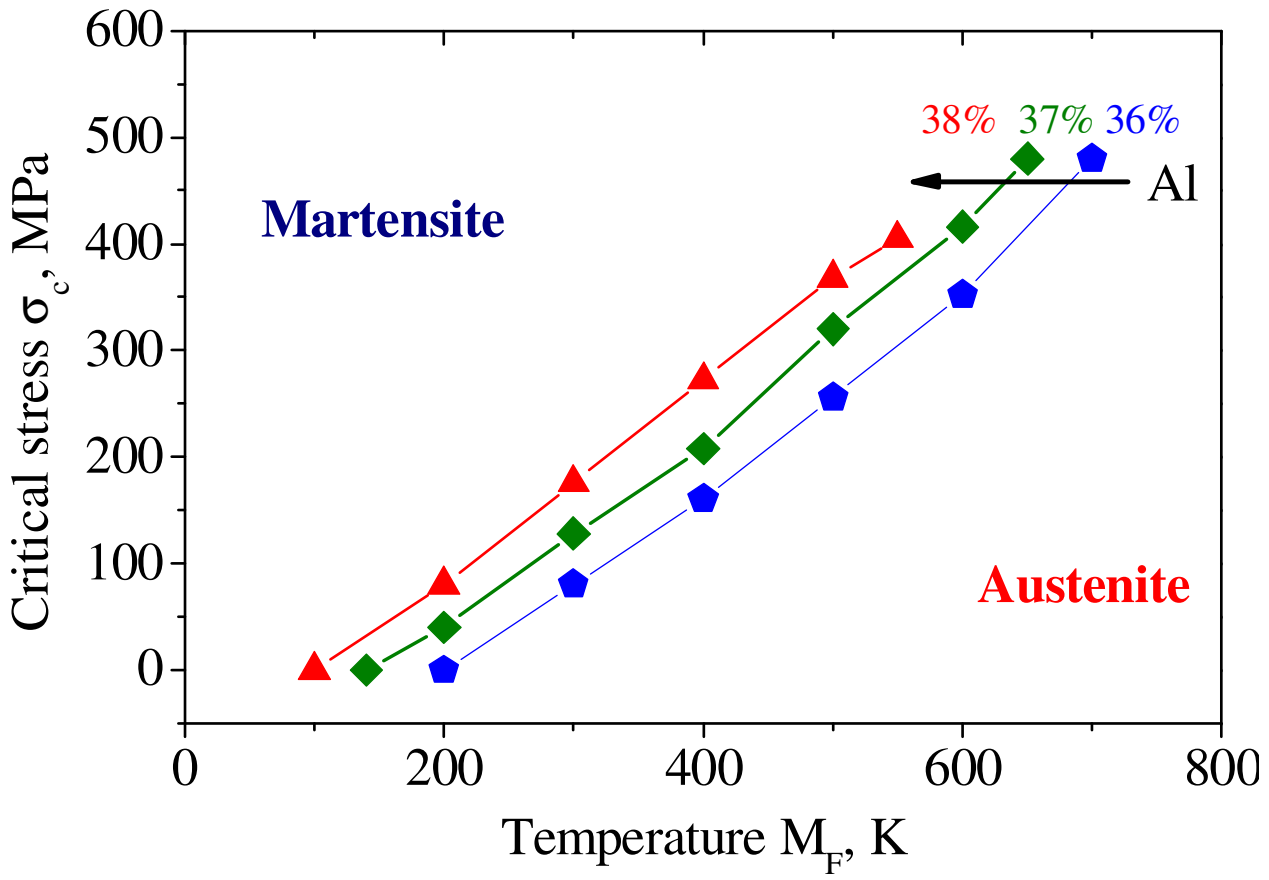

Entropy of harmonic system

$$S_{har} = -k_B \sum_j \ln(\hbar\omega_j / k_B T) + S_0$$

$$\Delta S_{AM} = -\int_0^\infty \ln(\omega)[g_A(\omega) - g_M(\omega)]d\omega = -\ln\frac{\overline{\omega}_A}{\overline{\omega}_M}$$

$$A_{VV}(t) = \int_0^\infty V(\tau)V(\tau + t)d\tau$$

$$g(\omega) = \frac{1}{2\pi}\int_0^\infty e^{-\omega t} A_{VV}(t)dt$$

Spectral densities in martensite

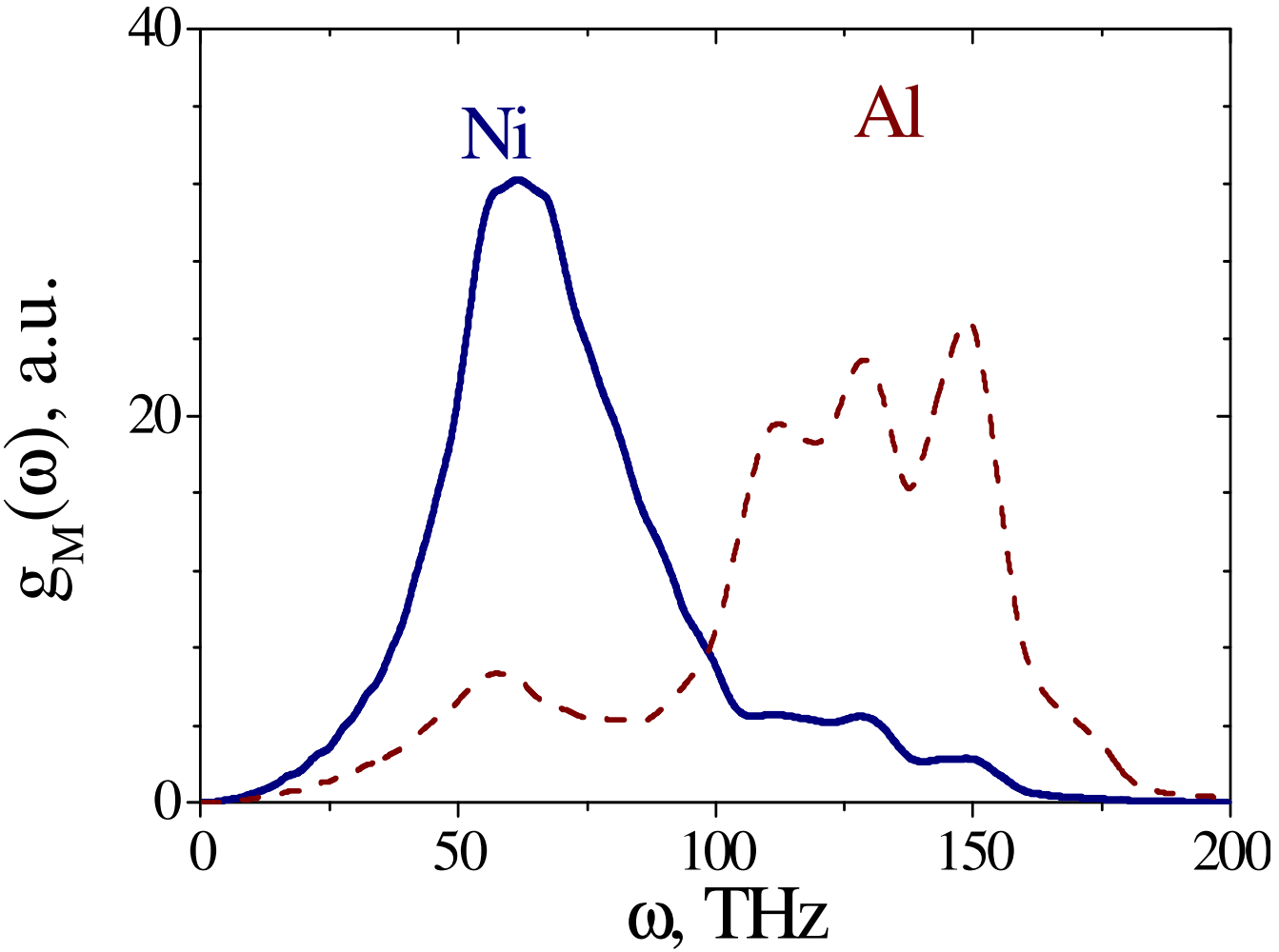

- *Low-frequency limit: ~ ω^2*

Spectral densities in austenite

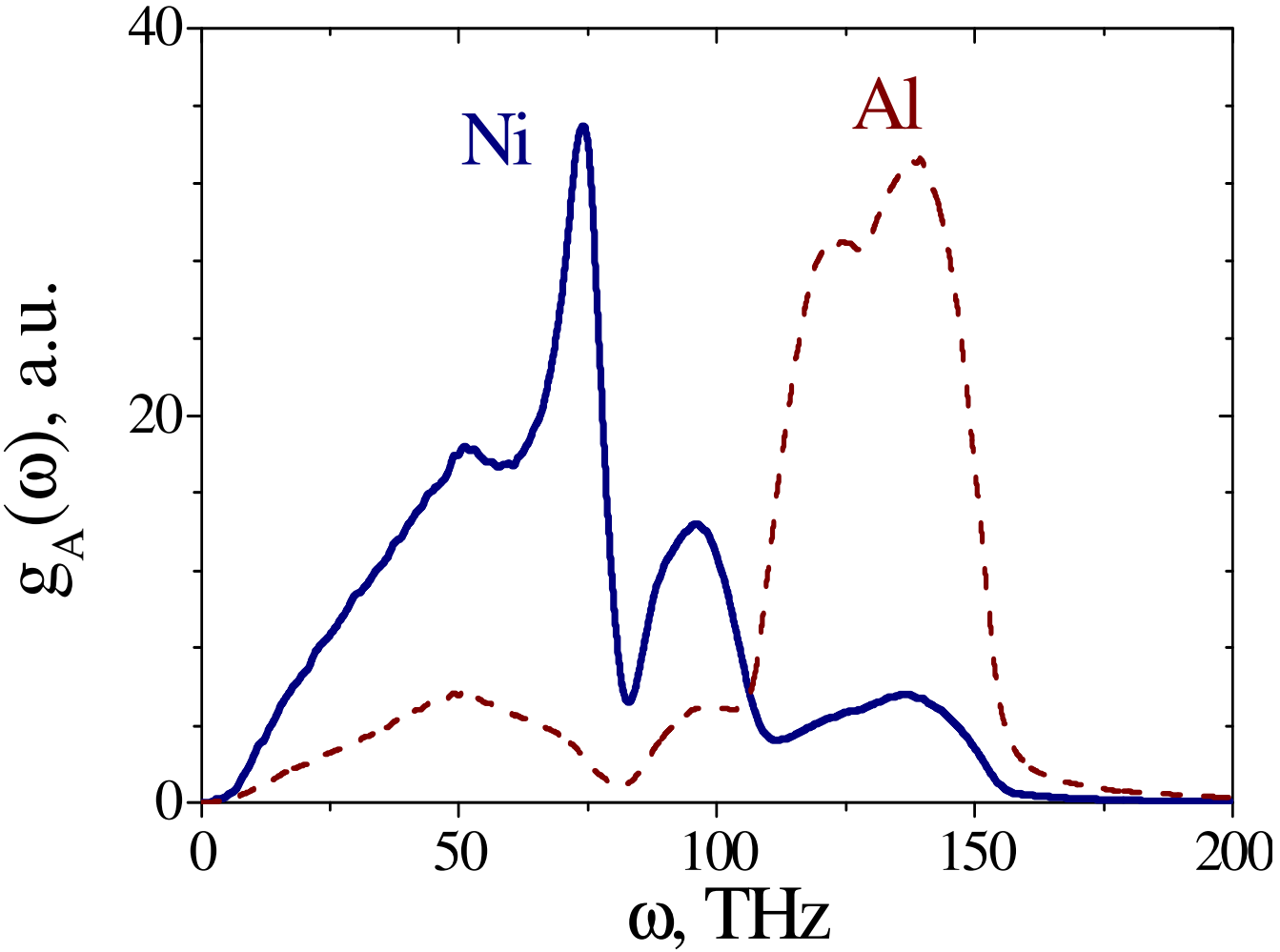

- *Soft modes at small ω ?*

Enthalpy difference, Ni-37%Al

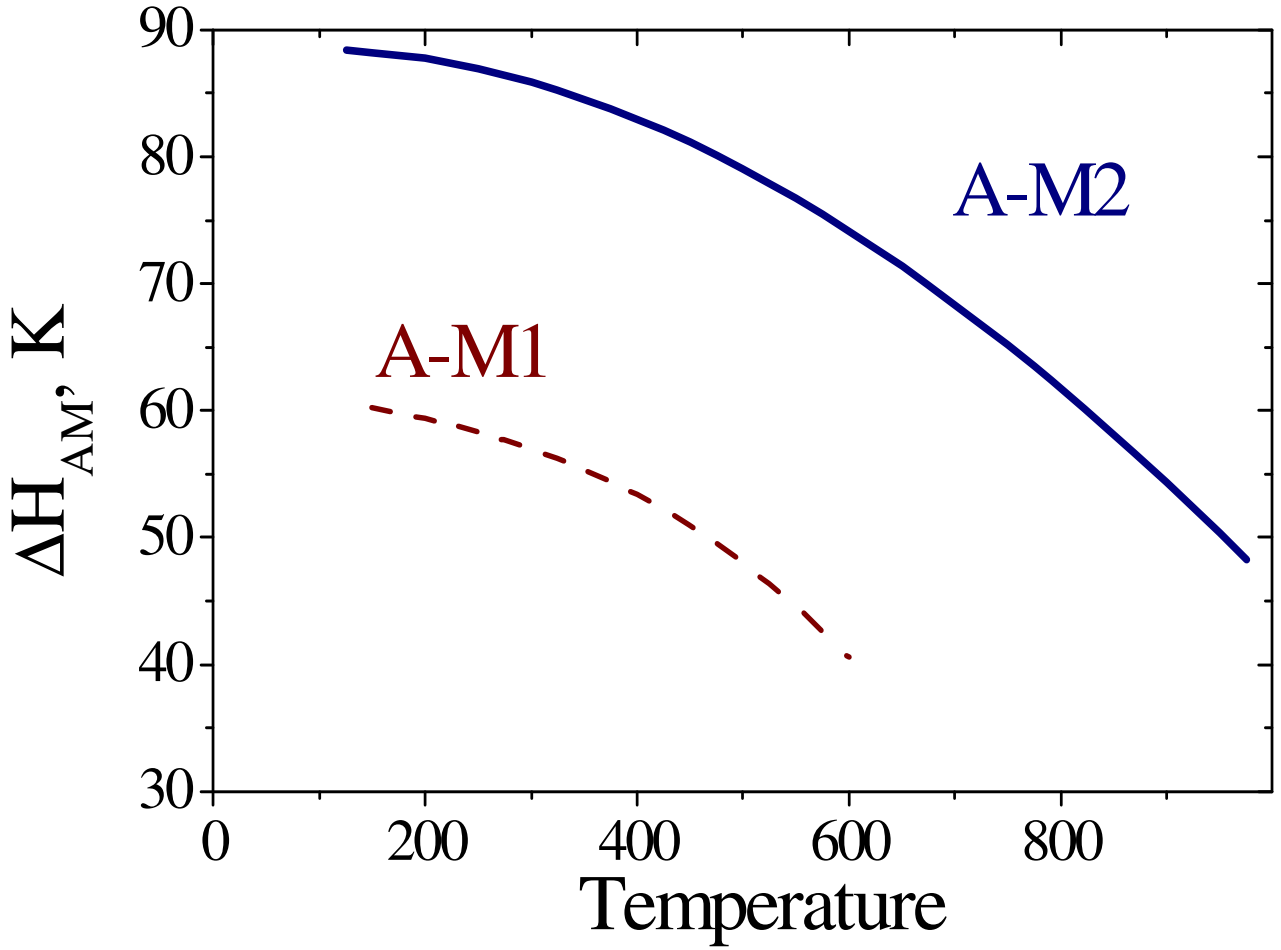

Free energy difference

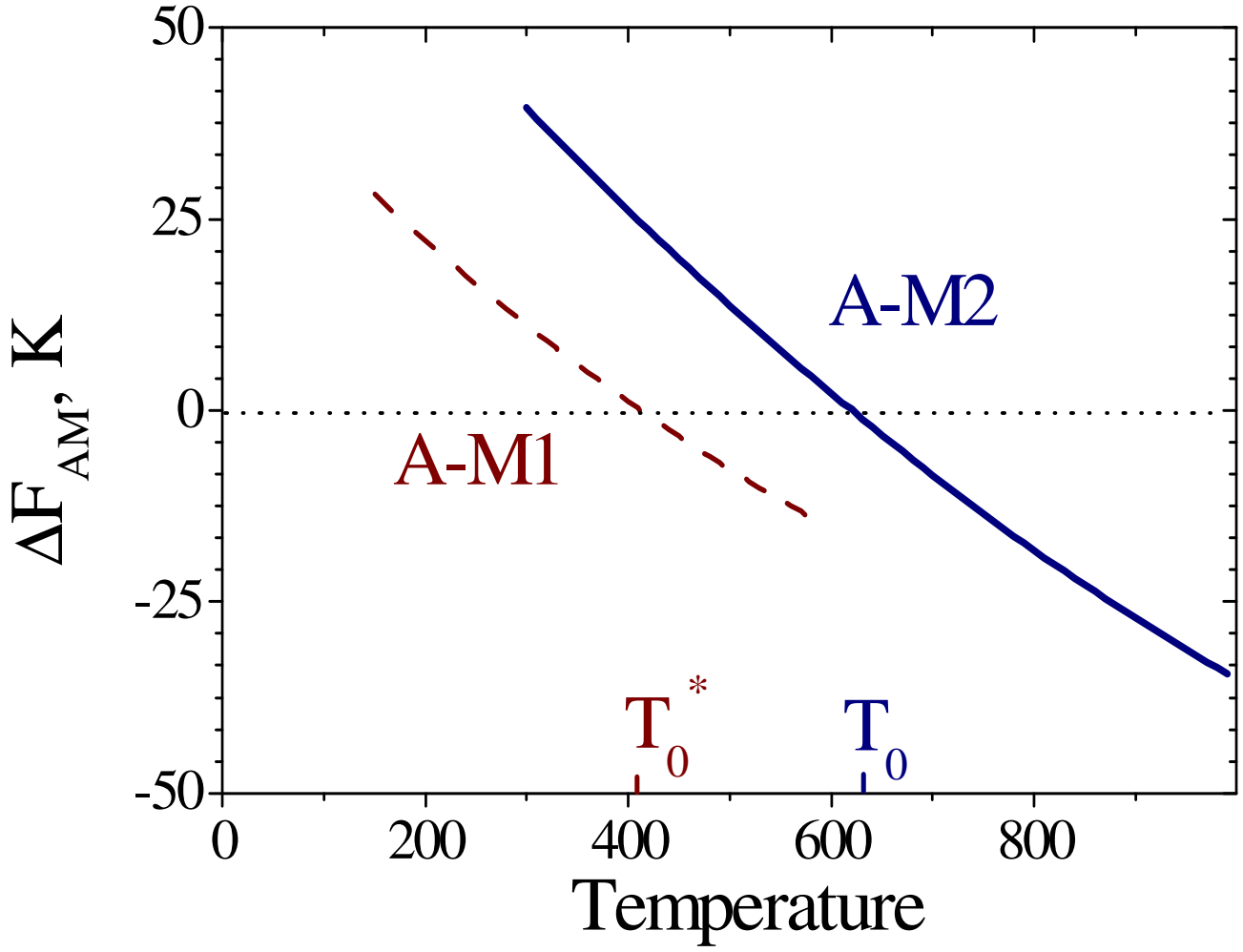

Radial Distribution Function

$$g(r) = \frac{V}{4\pi r^2 N^2} \left\langle \sum_i \sum_{j \neq i} \delta(r - r_{ij}) \right\rangle$$

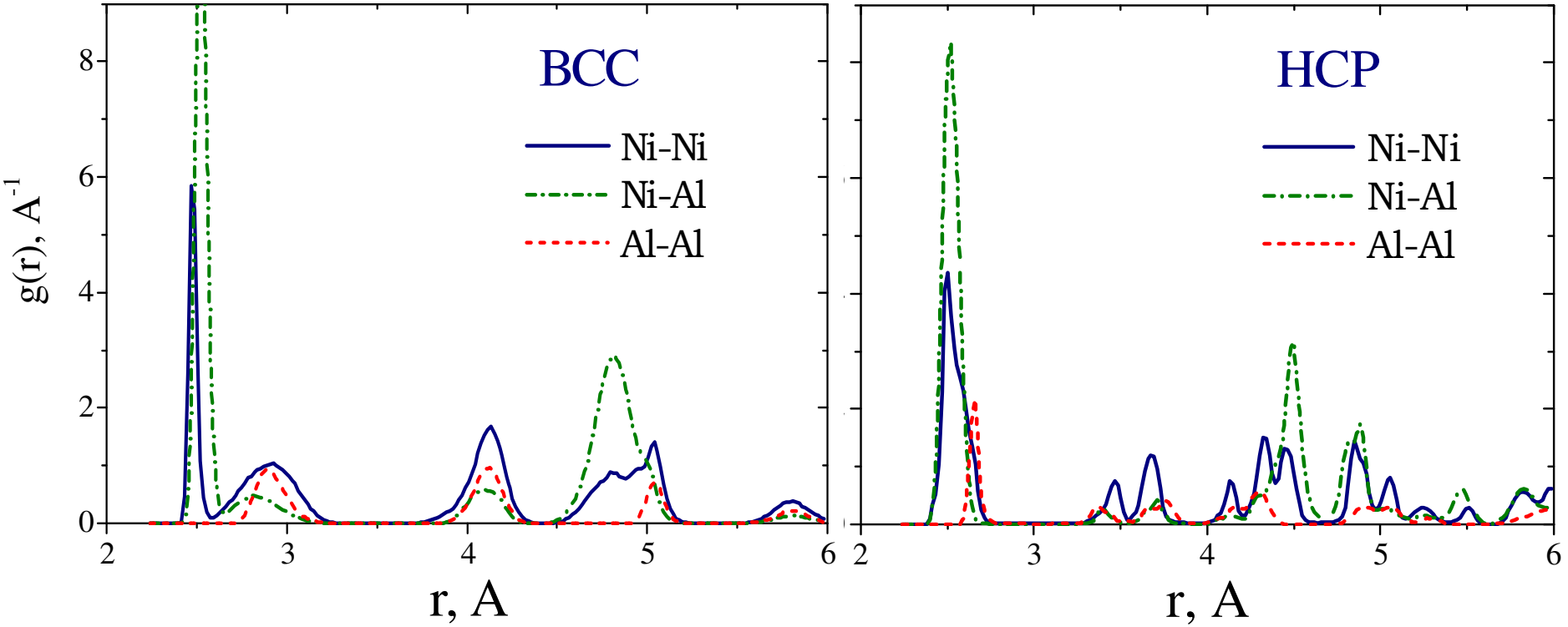

- BCC before MPT
- HCP after MPT

The Bainitic Ni_5Al_3 phase

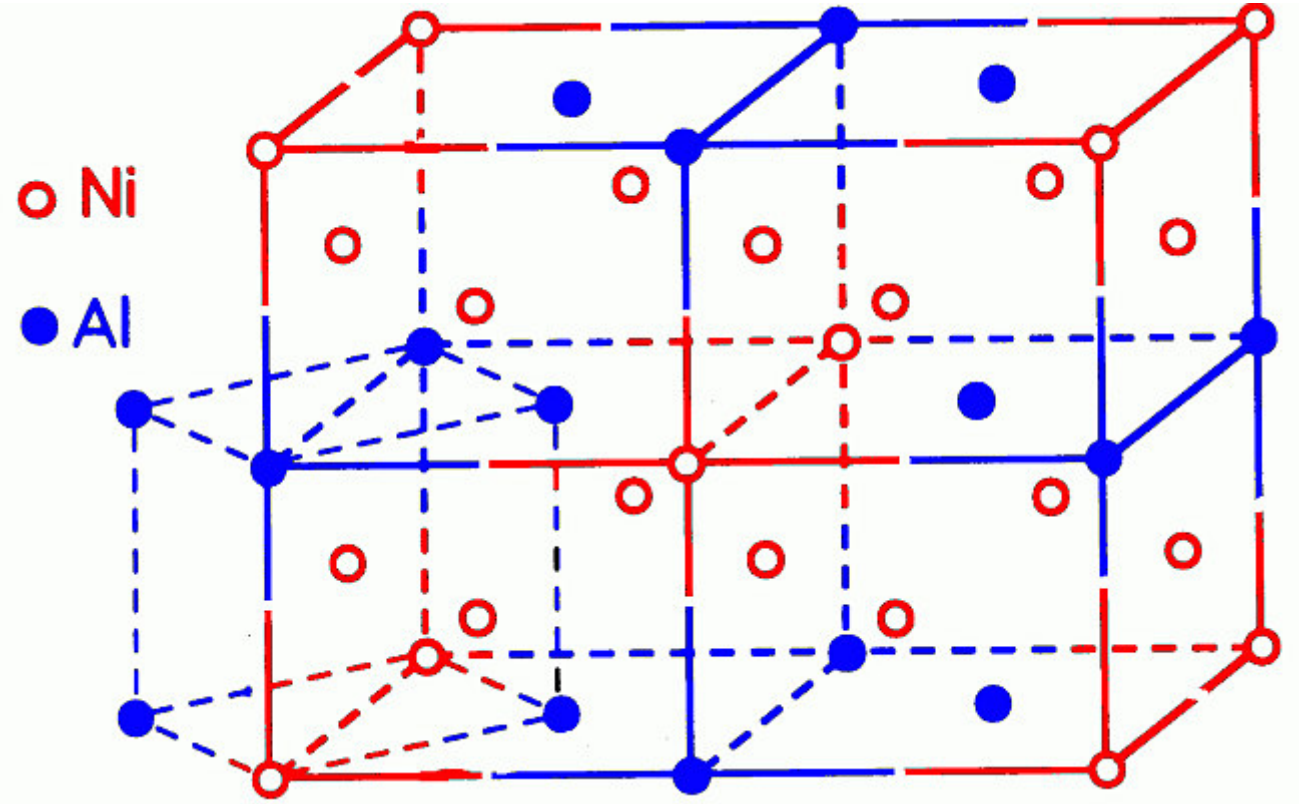

D. Schryvers et al,
J. de Physique IV, Vol. 5 (1995) Col. C8, p. 1029

MT in ordered alloy, Ni_5Al_3 (PBC): B→A →B

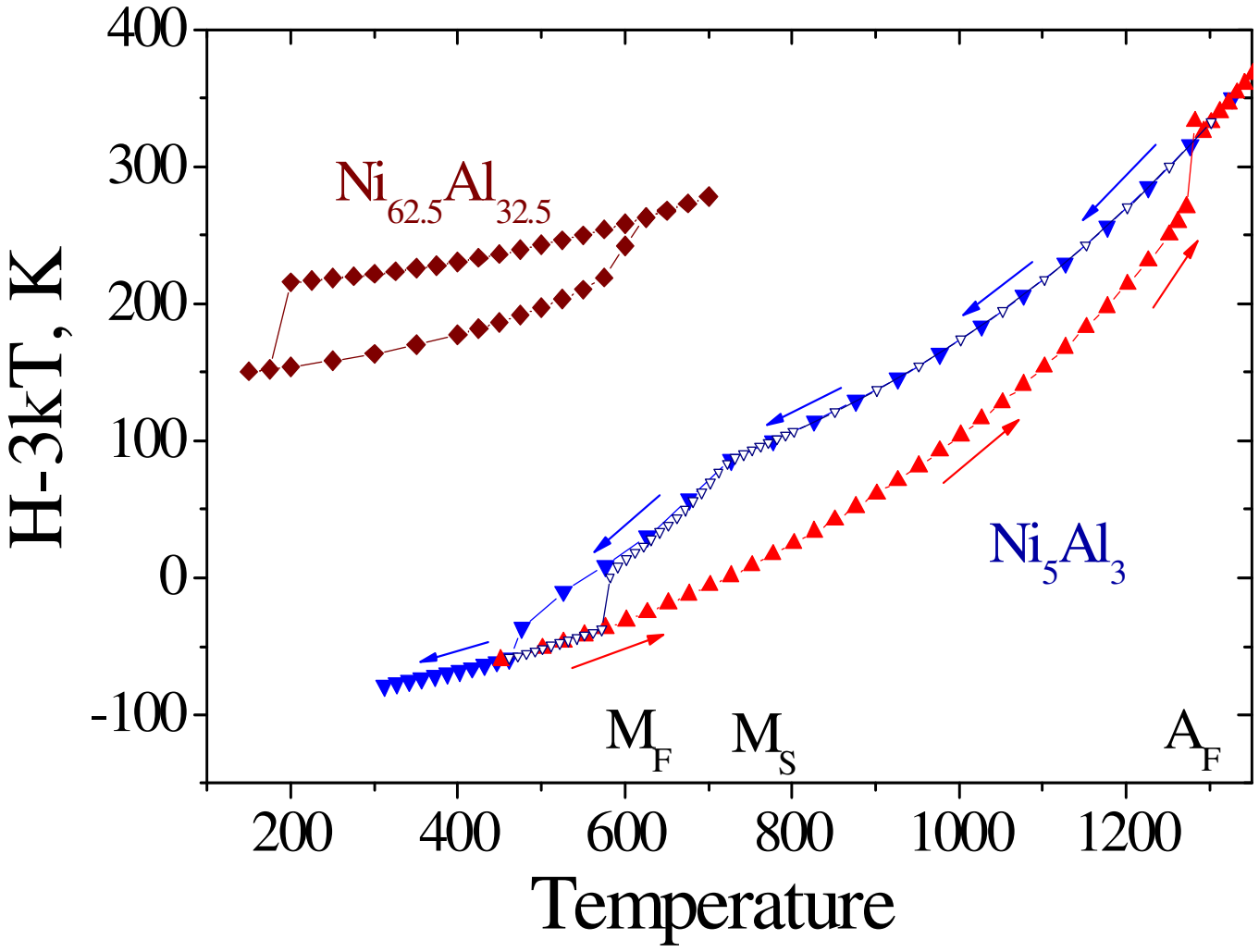

- *Compositional ordering facilitates to martensite (bainitic) phase*

Free external surface

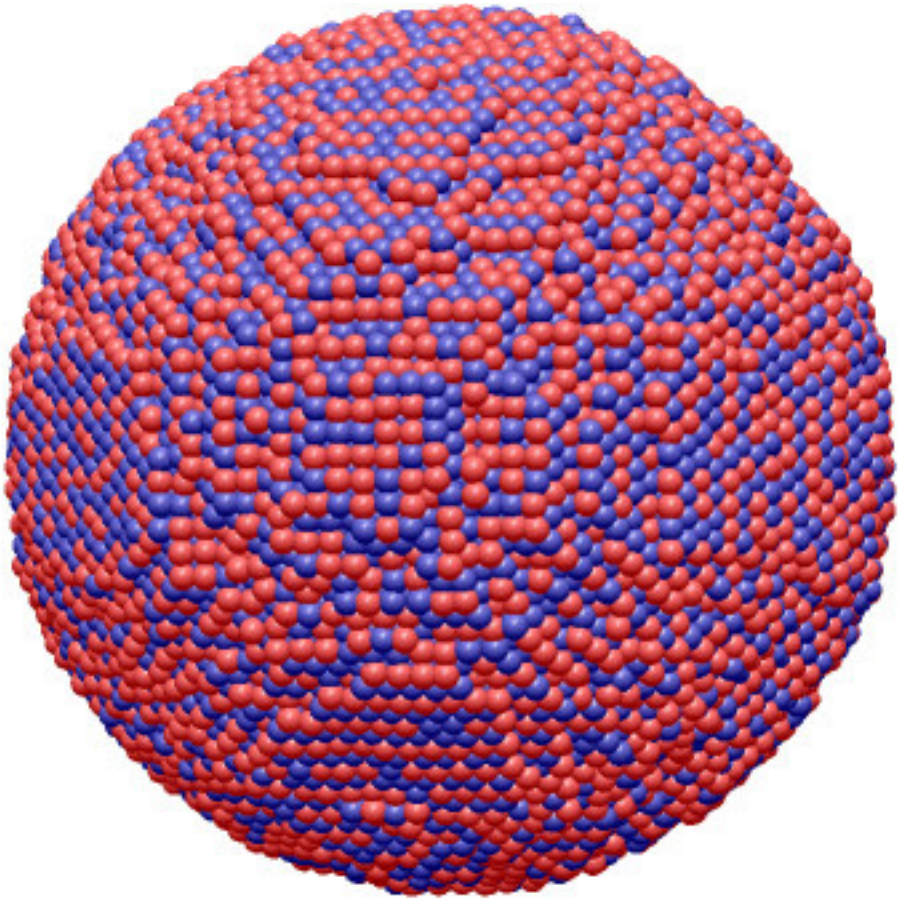

Ni62-Al38

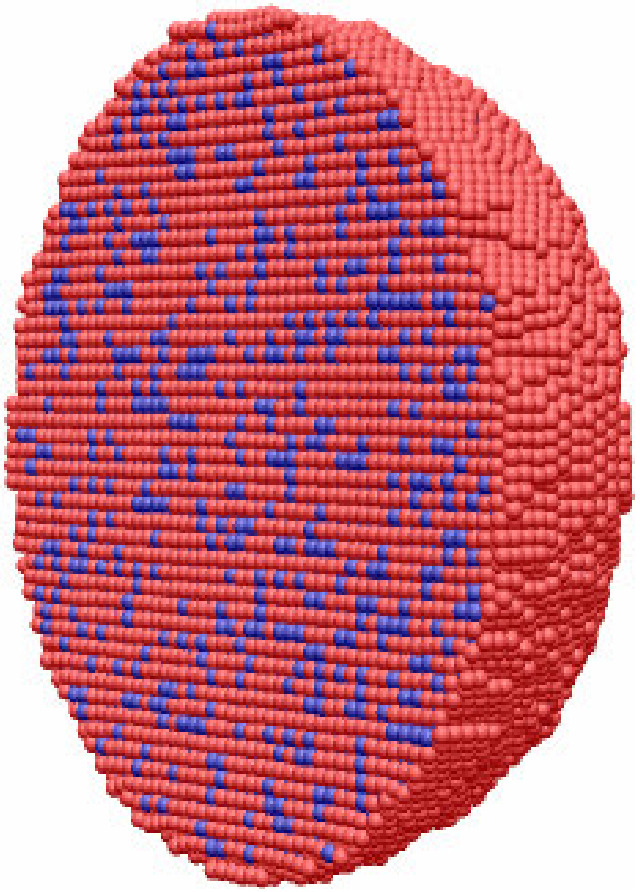

Al-Enriched

MT in finite-size Ni_5Al_3 : B→A →B

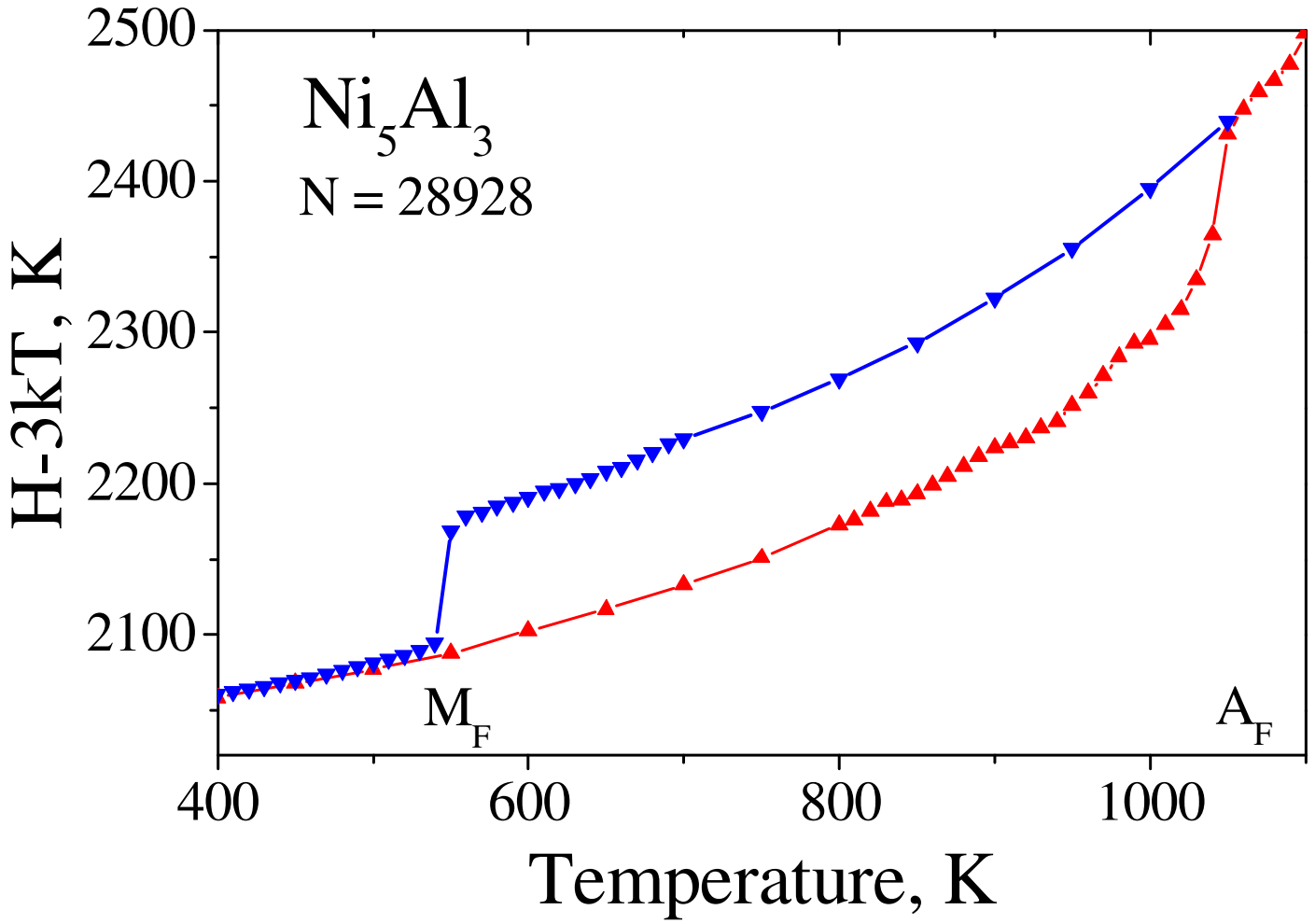

Dynamics of transformation A →B in Ni_5Al_3

T = 635K
N = 134048

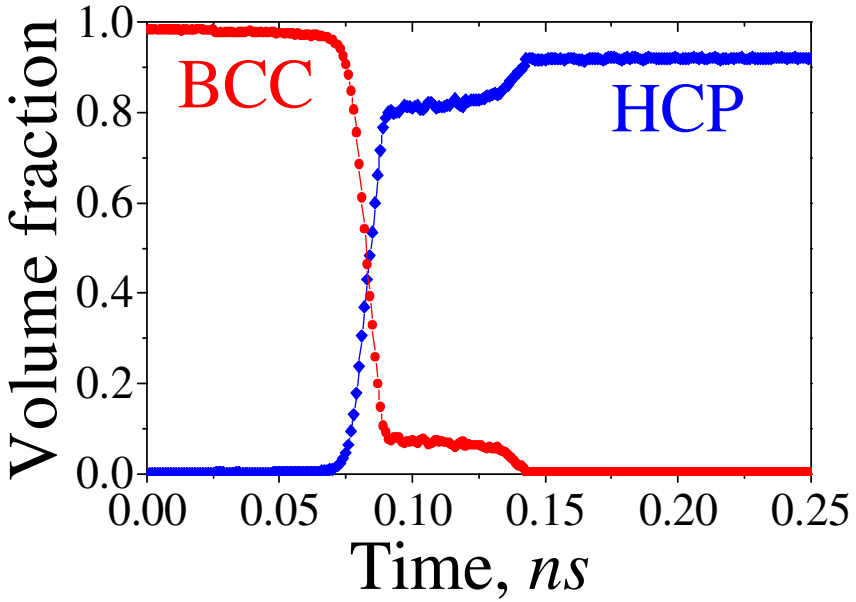

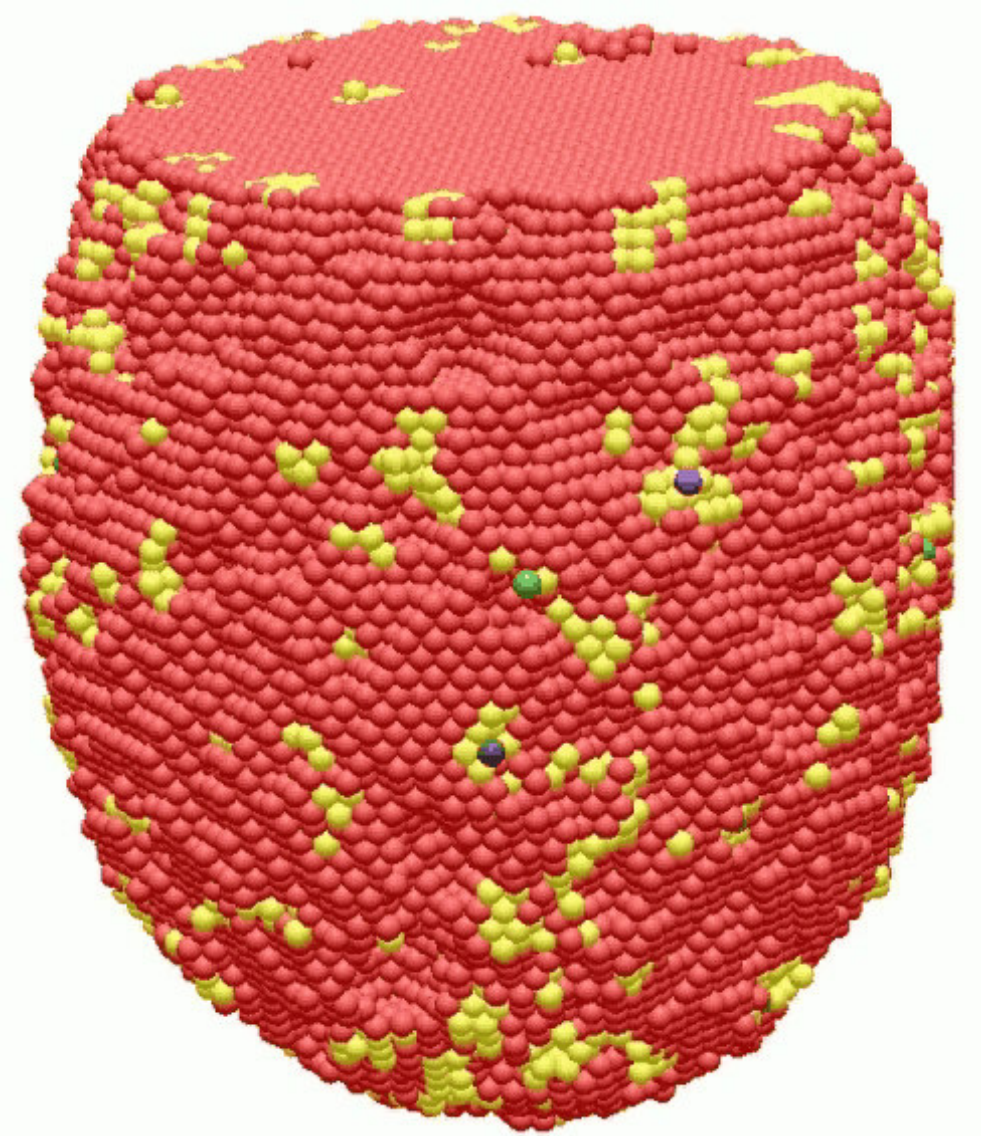

MT in finite-size ordered Ni_5Al_3 and Ni_7Al_5

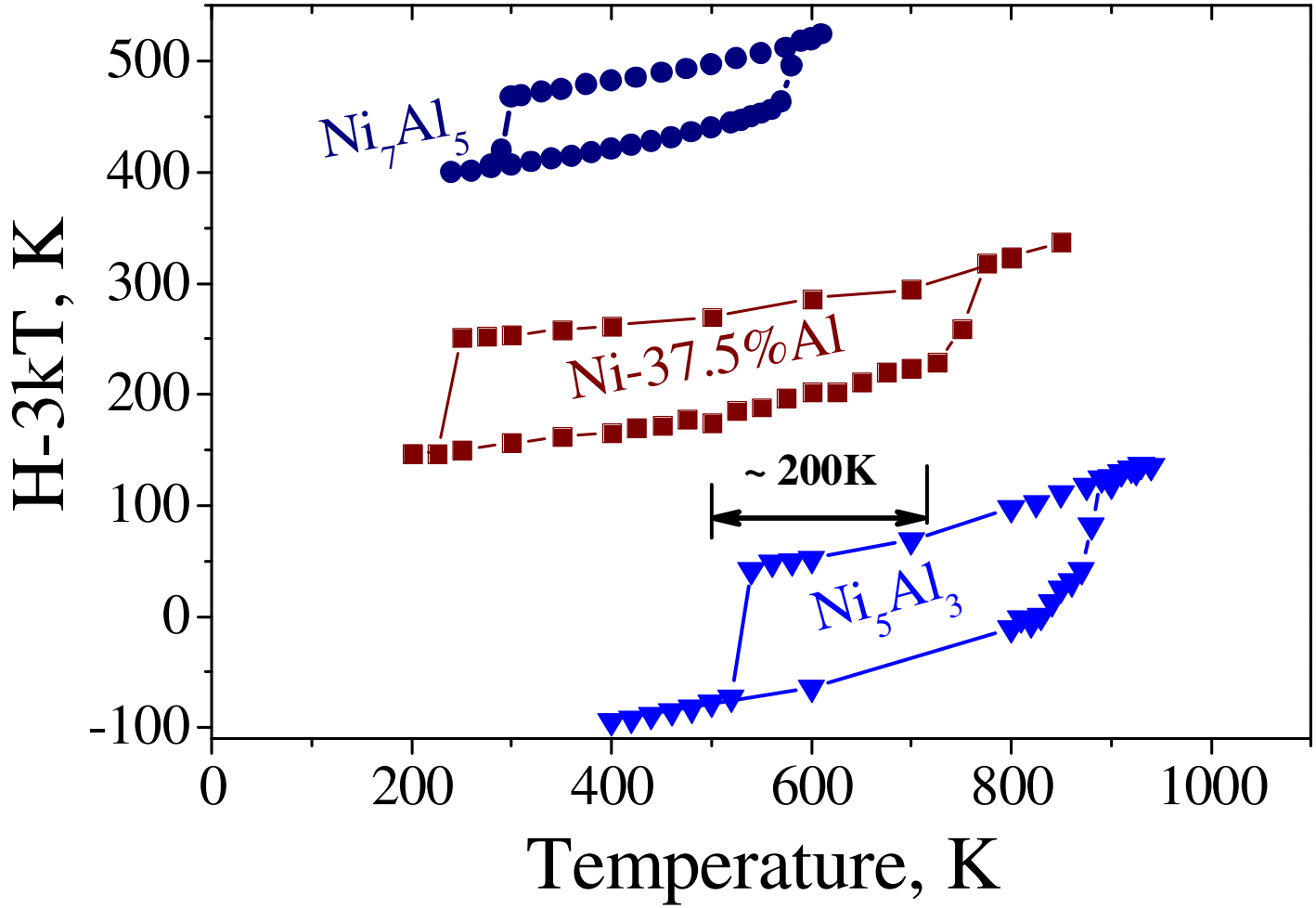

- *Composition disorder decreases transformation temperature up to ~200K*

MT in finite-size ordered Ni_7Al_5

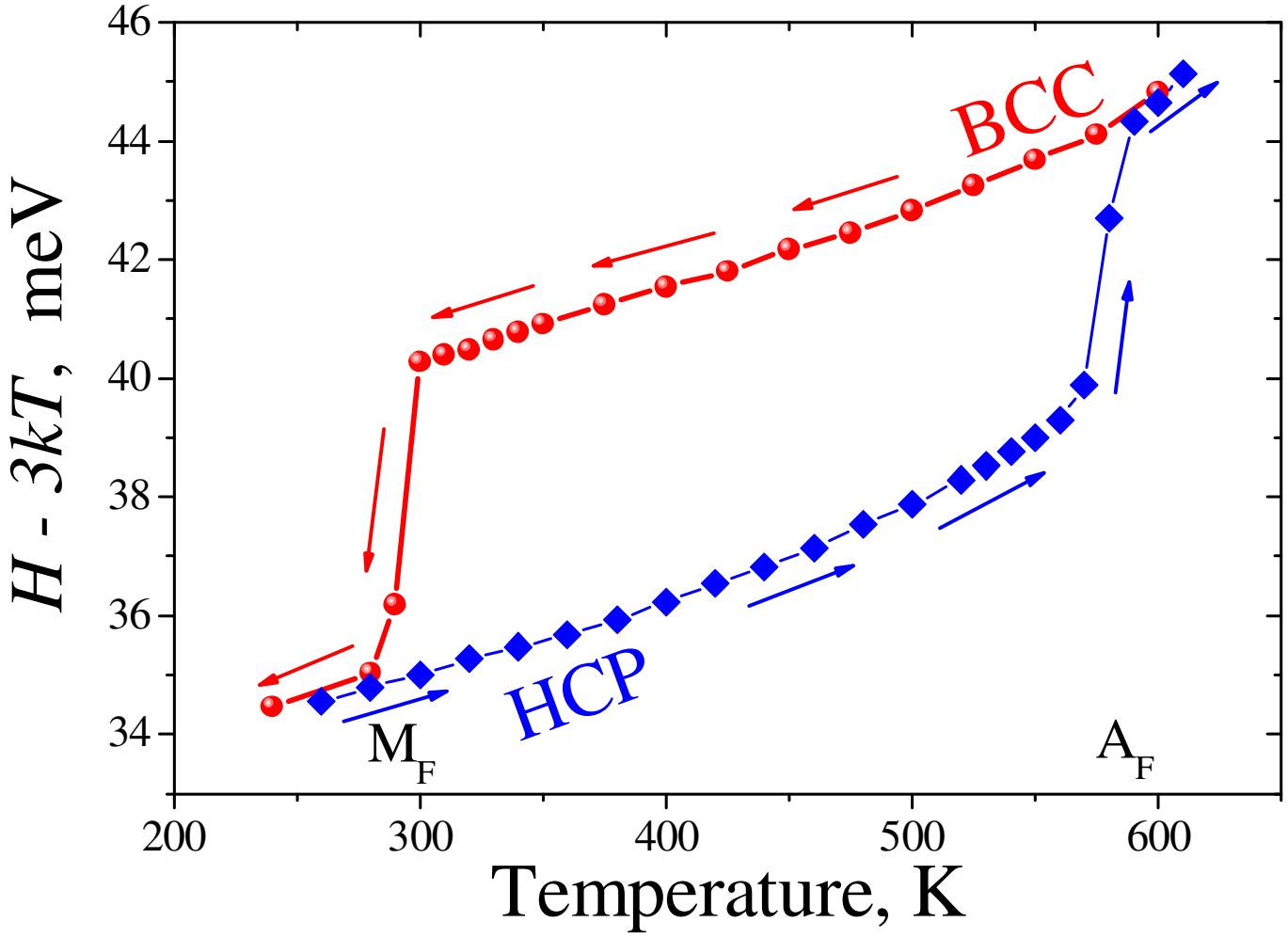

- *The 1-st order phase transformations: $A \rightarrow M \rightarrow A$*

Homogeneous transformation A → M

Ni_7Al_5

T = 290K, N = 390948

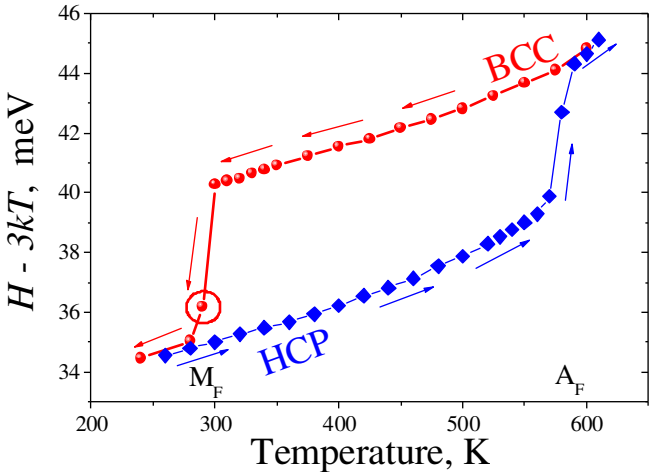

Perfect FCC+HCP
Distorted FCC+HCP
Perfect BCC
Distorted BCC
Perf. & Dist. ICO
Unclassified

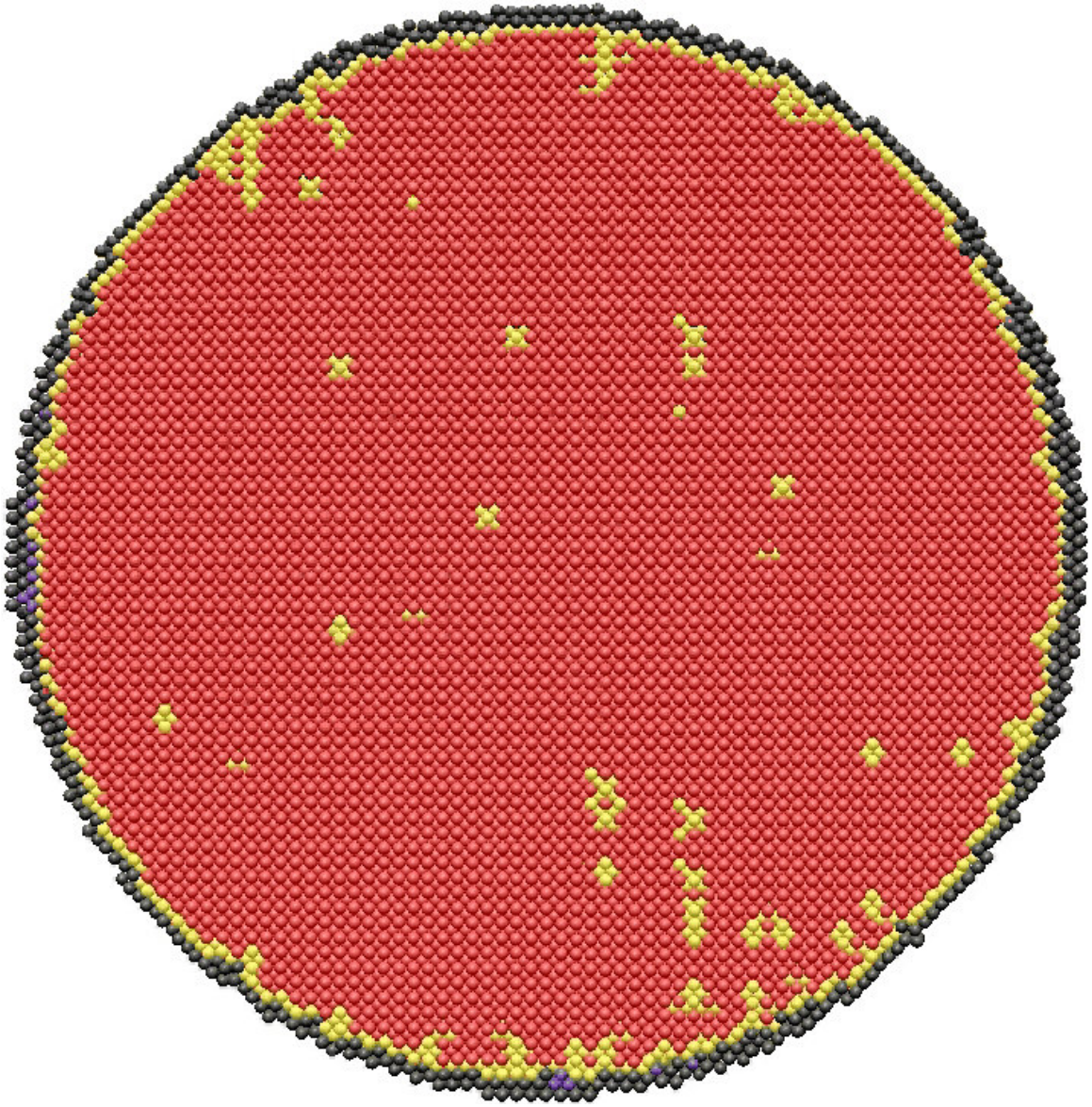

Heterogeneous transformation M → A

Ni_7Al_5

T = 580K, N = 1809648

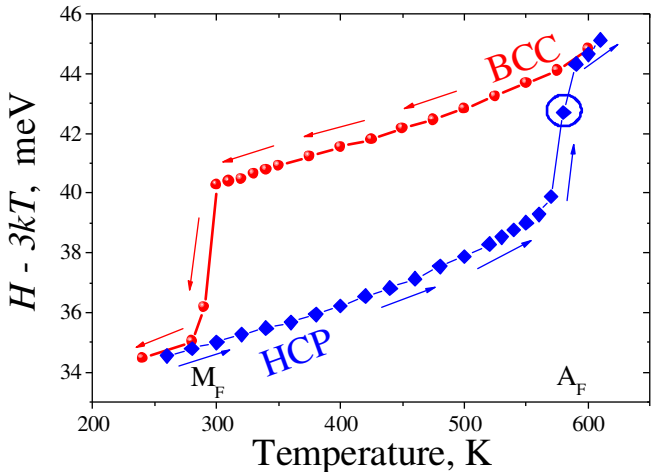

Perfect FCC+HCP
Distorted FCC+HCP
Perfect BCC
Distorted BCC
Perf. & Dist. ICO
Unclassified

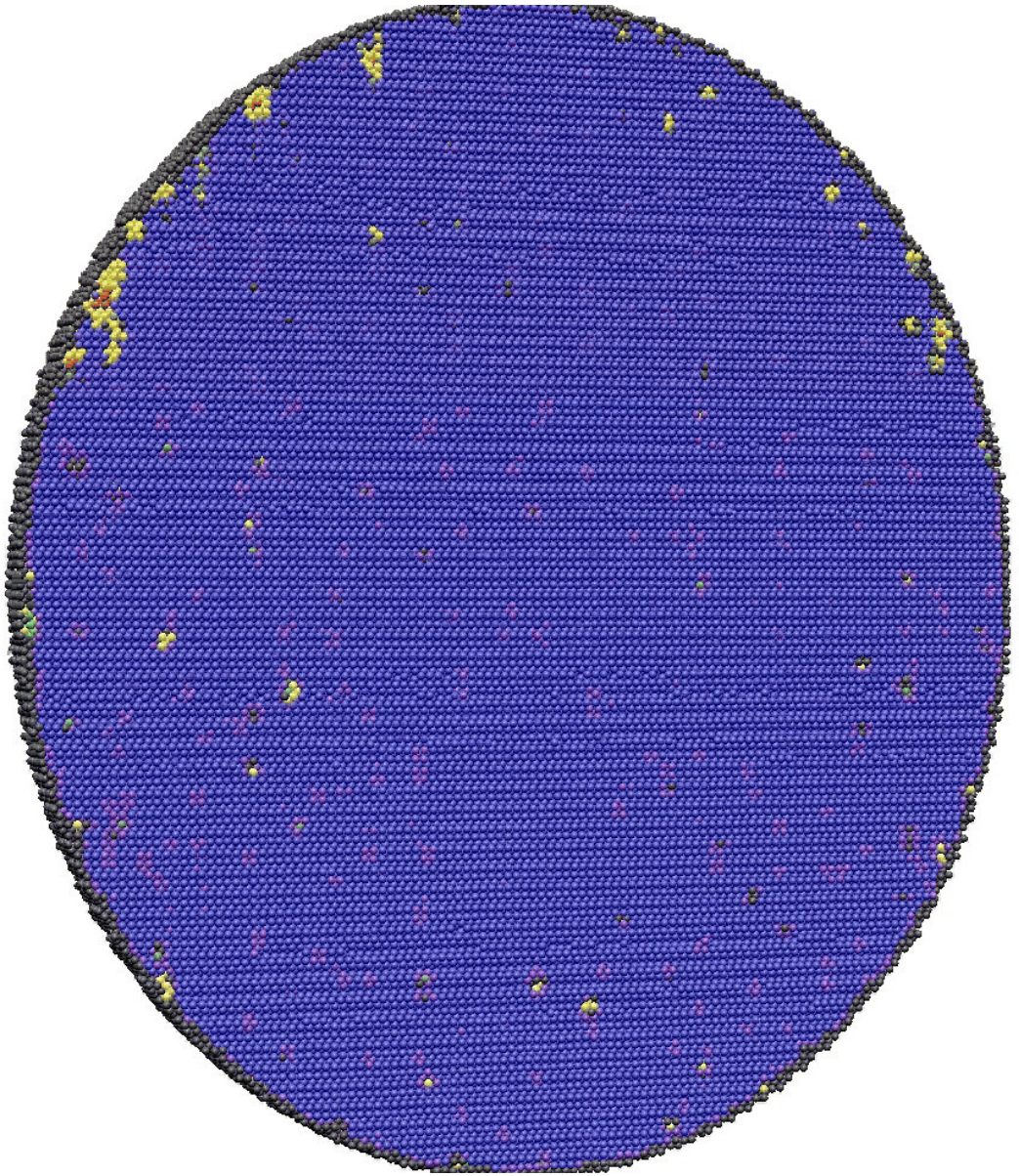

Grain boundary preparation

Cutting of init sphere

Cross-section of final state

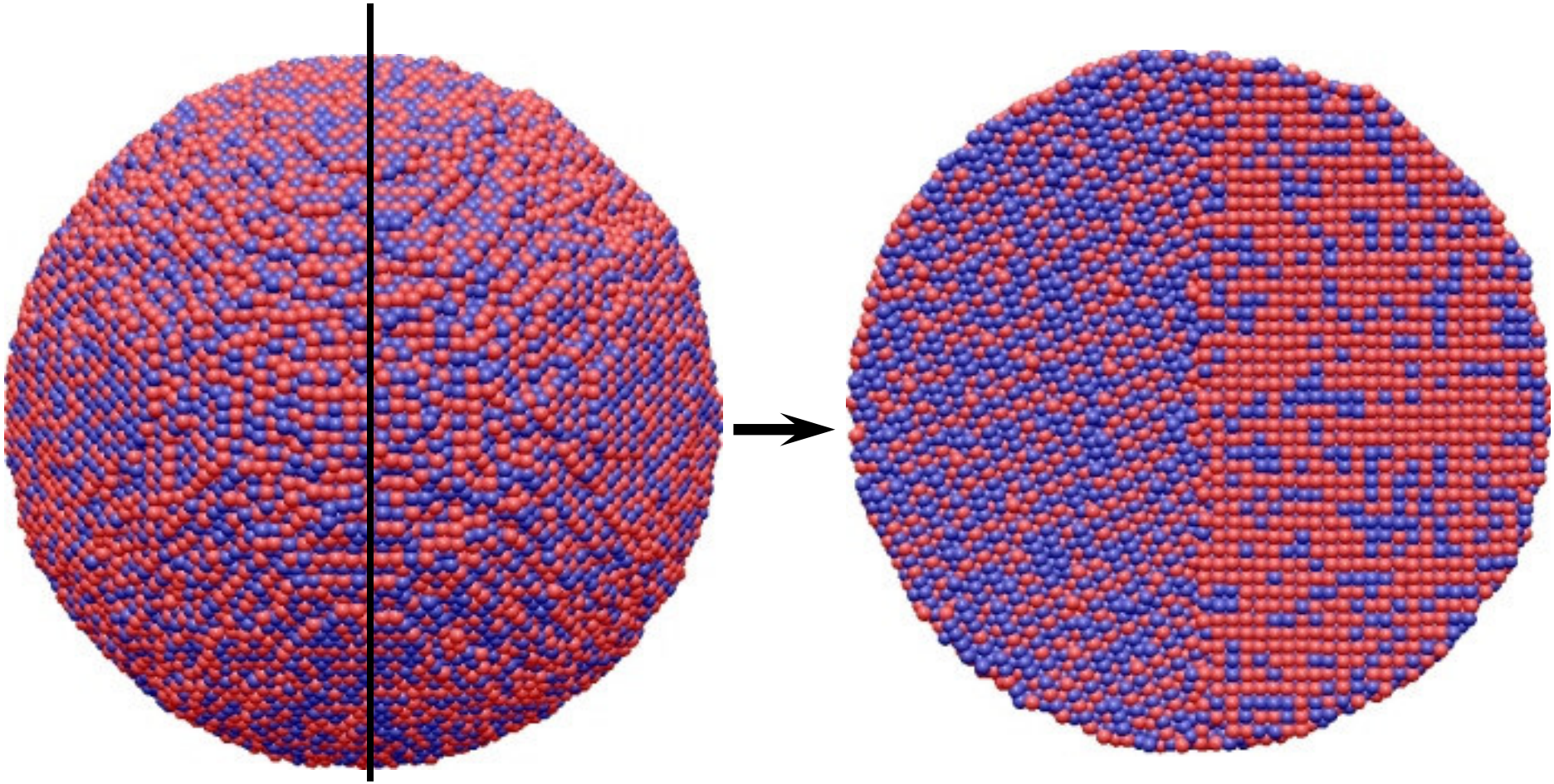

Grain boundary effect

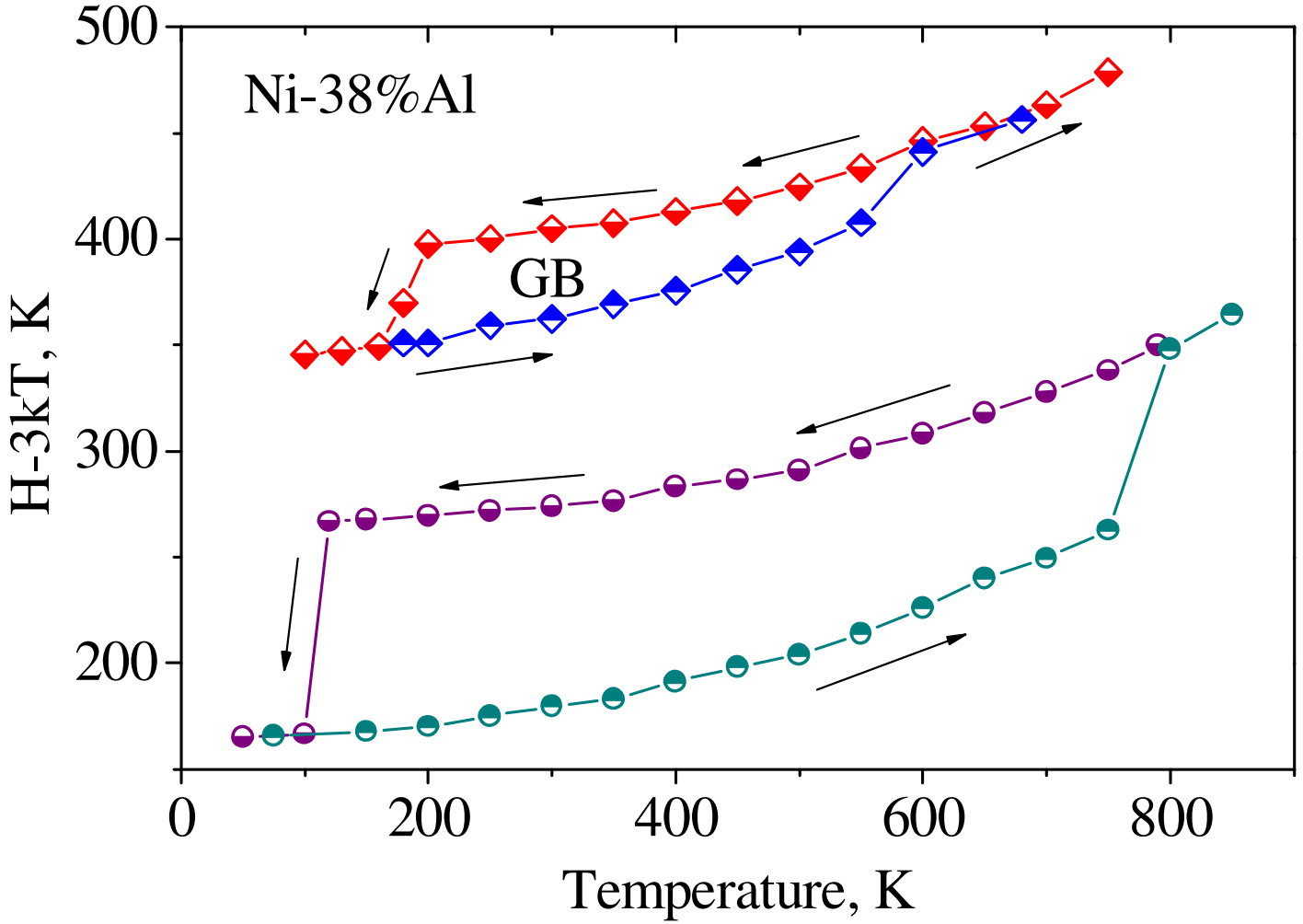

A→M heterogeneous transformation near GB

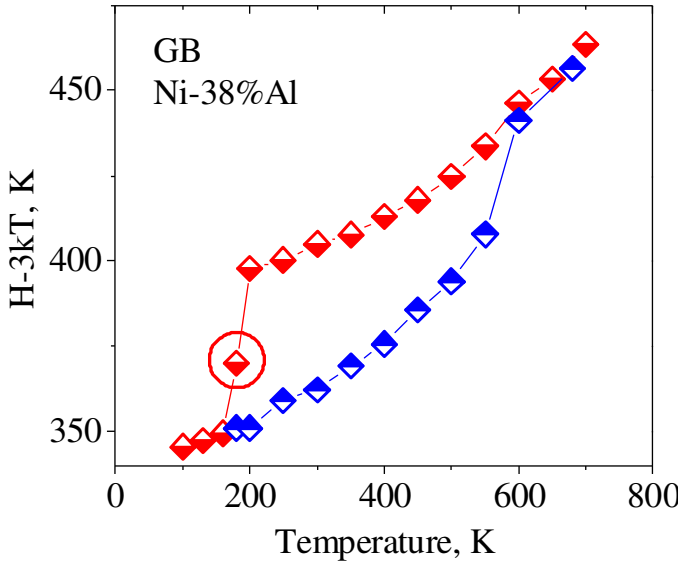

N = 130995

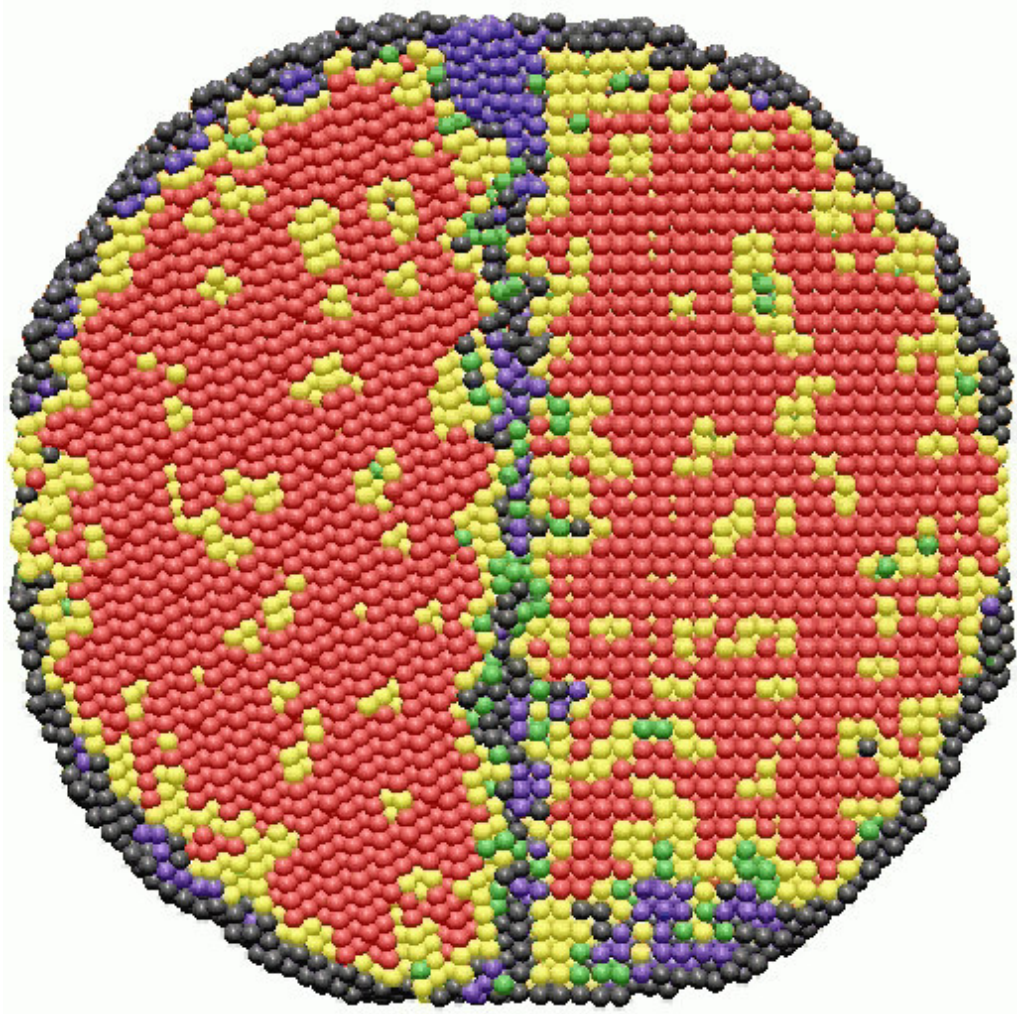

Perfect FCC + HCP
Distorted FCC + HCP
Perfect BCC
Distorted BCC
Perf. & Dist. ICO
Unclassified

T = 180 K

A→M heterogeneous transformation near GB

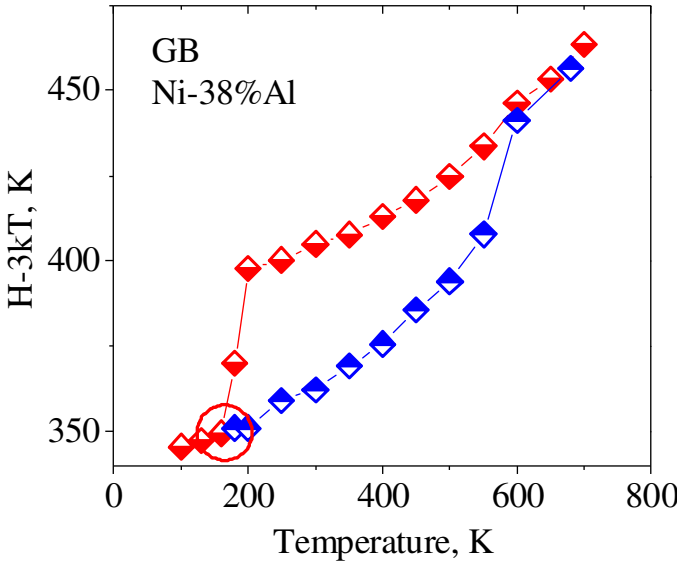

N = 130995

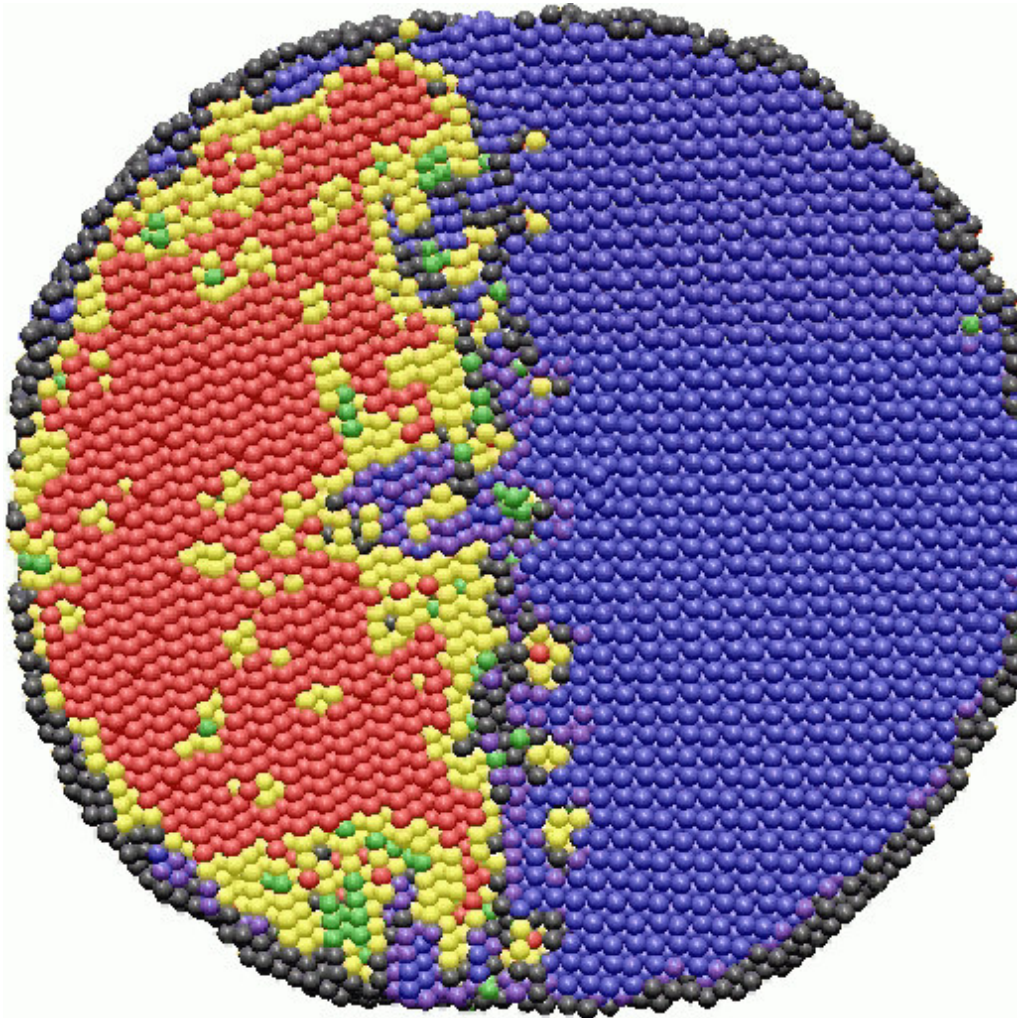

Perfect FCC + HCP
Distorted FCC + HCP
Perfect BCC
Distorted BCC
Perf. & Dist. ICO
Unclassified

T = 160 K

M→A heterogeneous transformation near GB

N = 130995

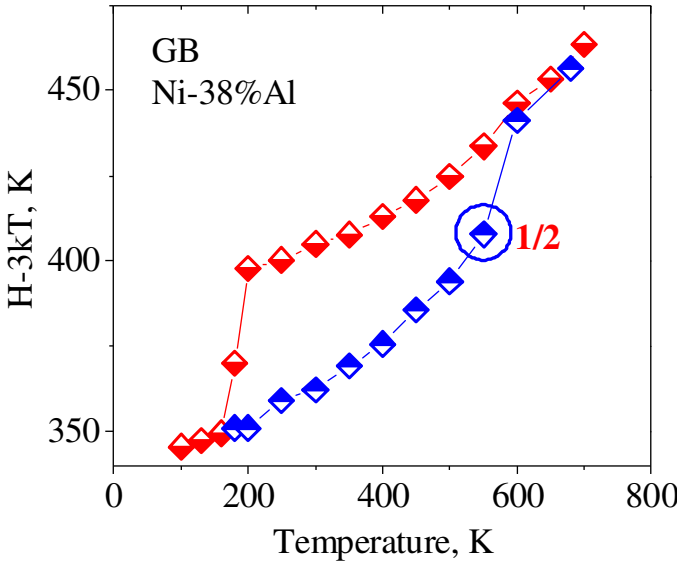

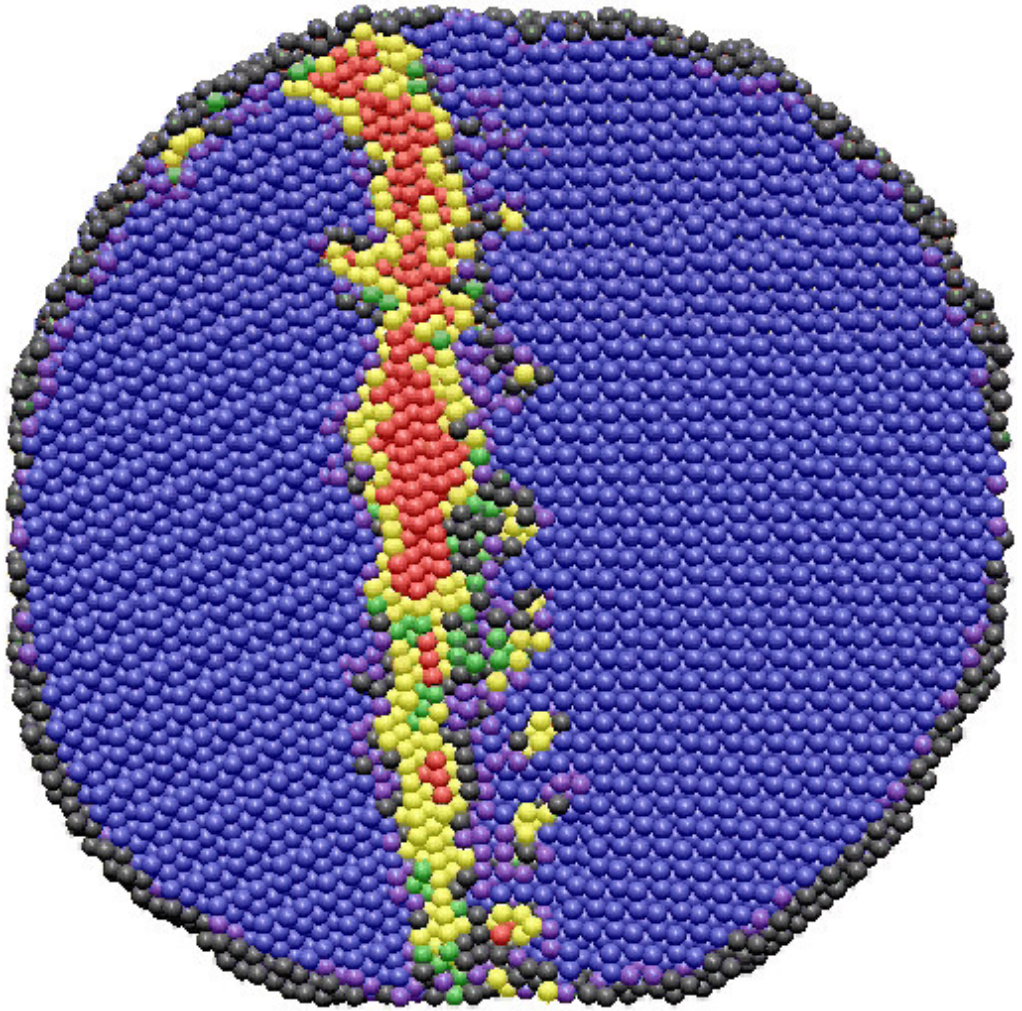

Perfect FCC + HCP
Distorted FCC + HCP
Perfect BCC
Distorted BCC
Perf. & Dist. ICO
Unclassified

T = 550 K

M→A heterogeneous transformation near GB

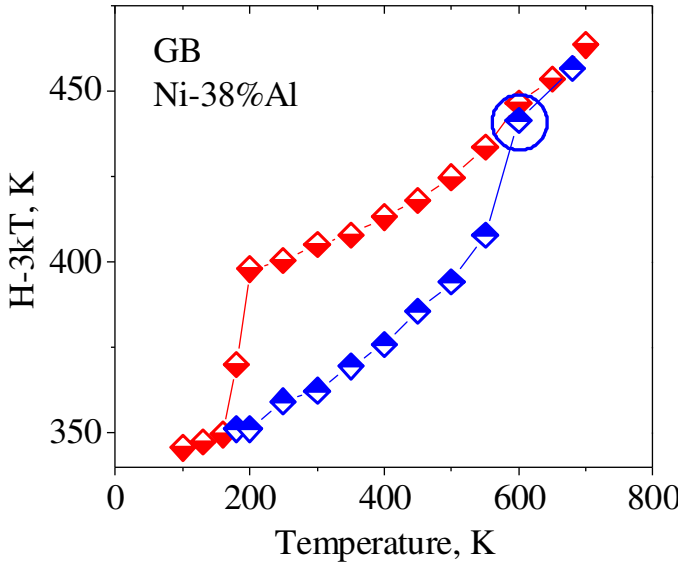

N = 130995

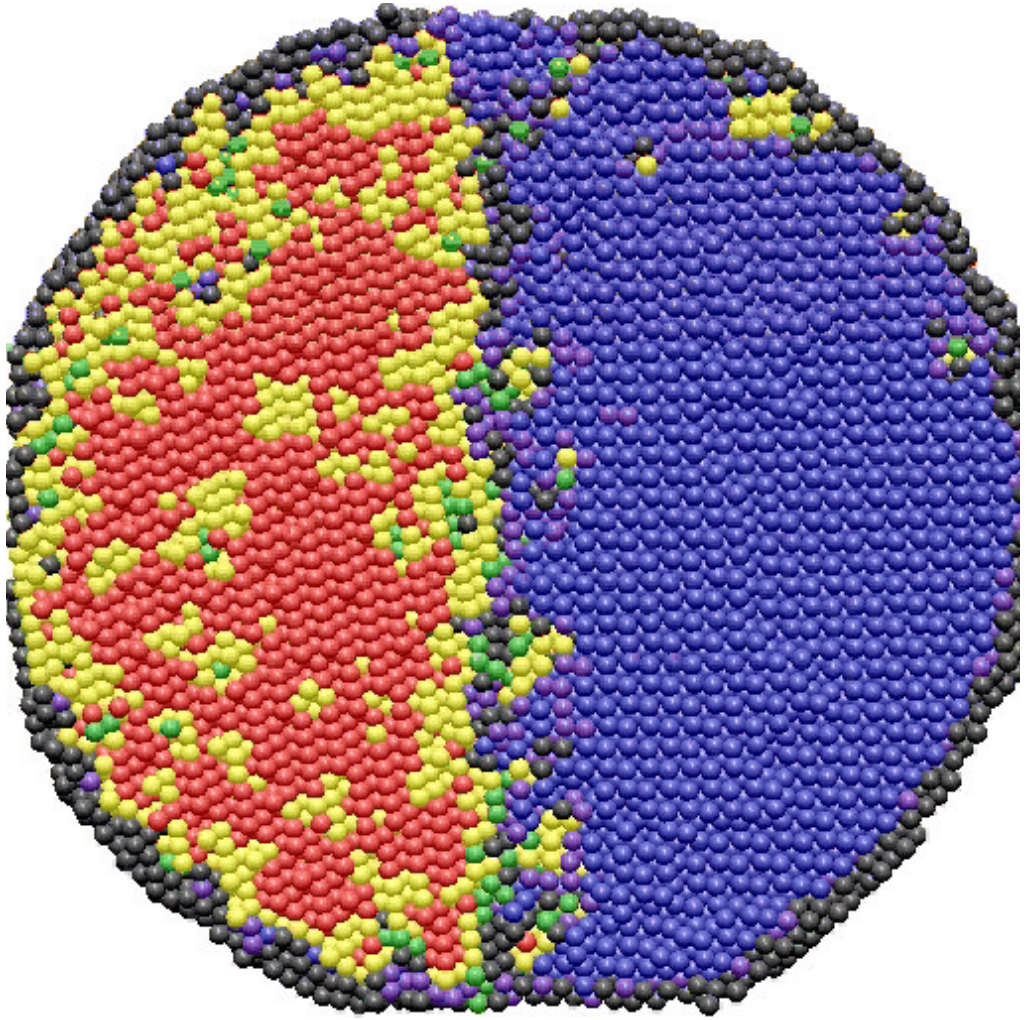

Perfect FCC + HCP
Distorted FCC + HCP
Perfect BCC
Distorted BCC
Perf. & Dist. ICO
Unclassified

T = 600 K

Atomistic simulation of track

Electronic system: Spike Model

$$C_e(T_e)\frac{\partial T_e}{\partial t} = \frac{1}{r}\frac{\partial}{\partial r} rK_e(T_e)\frac{\partial}{\partial r}T_e - g(T_e - T_a)$$

$$T_e(r,0) = T_e^0 \exp(-r^2 / 2r_0^2)$$

$$\kappa_e = K_e / C_e$$

$dE/dx = 25$ keV/nm , $r_0 = 10$Å :

$$T_e^0 \sim 10^6 K$$

Atomic system: MD

$$m_i\dot{\vec{v}}_i = \vec{F}_i + m_i\gamma\left(\frac{T_e(r)}{T_a(r)} - 1\right)\vec{v}_i$$

$$T_a(r) = \frac{2}{3k_B N_r}\sum_{r-\delta<r_i<r+\delta}\frac{m_i\vec{v}_i^2}{2}$$

$$\frac{dT_a}{dt} = 2\gamma(T_e - T_a)$$

Simulation setup A

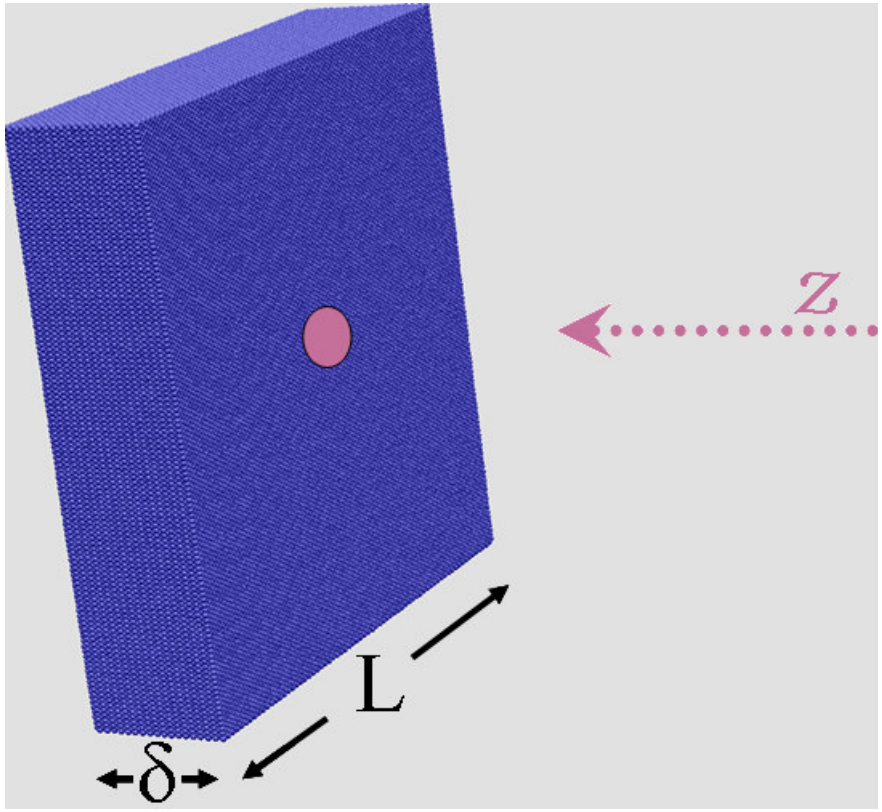

Ni-40%Al

δ = 7-10 *nm*

L = 30-40 *nm*

N = (0.6-1.4) $\cdot 10^6$

T = 300 K

Temperature development around track

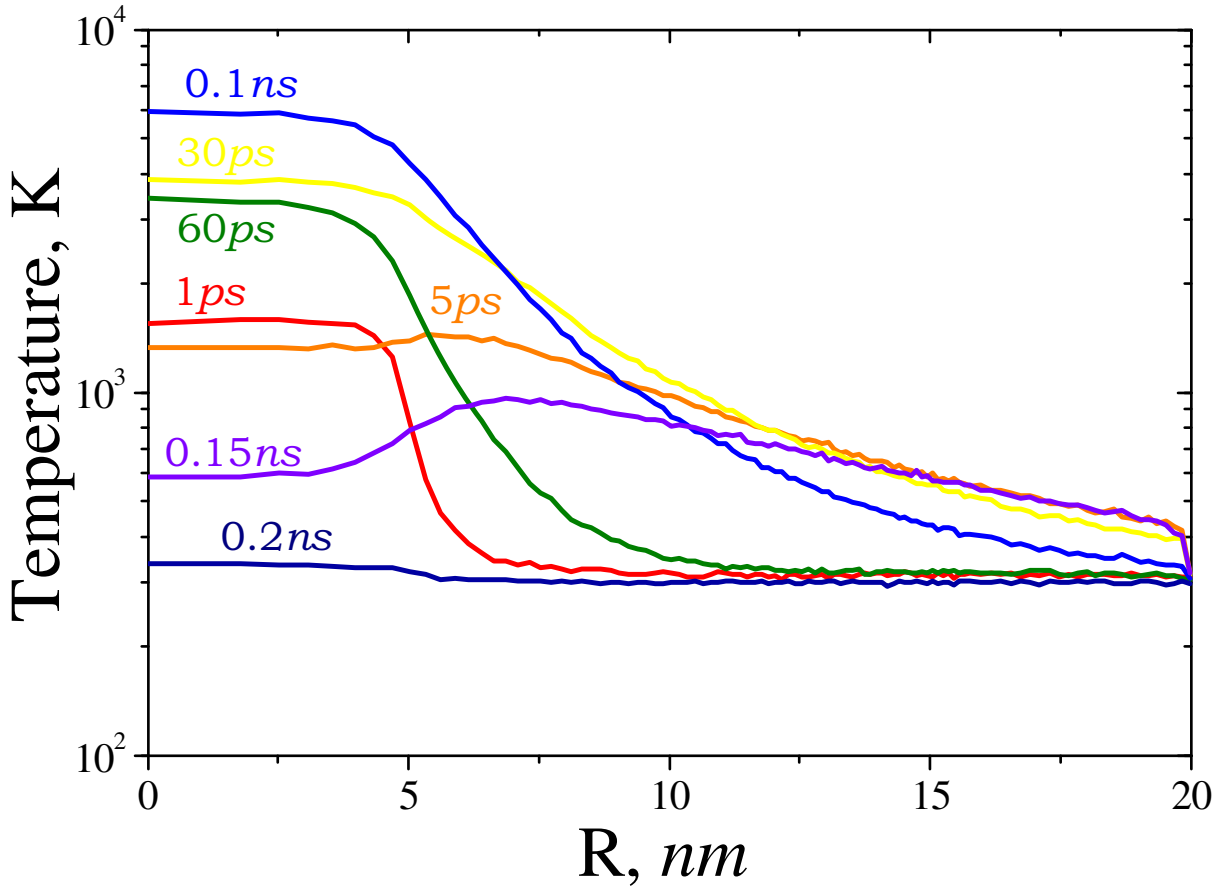

Phases Development in the Range of Swift Ion track

Ni - 40%Al

N = 1 400 000

T = 300 K

Perfect FCC + HCP
Distorted FCC + HCP
Perfect BCC
Distorted BCC
Perf. & Dist. ICO
Compositionally Disordered
Unclassified

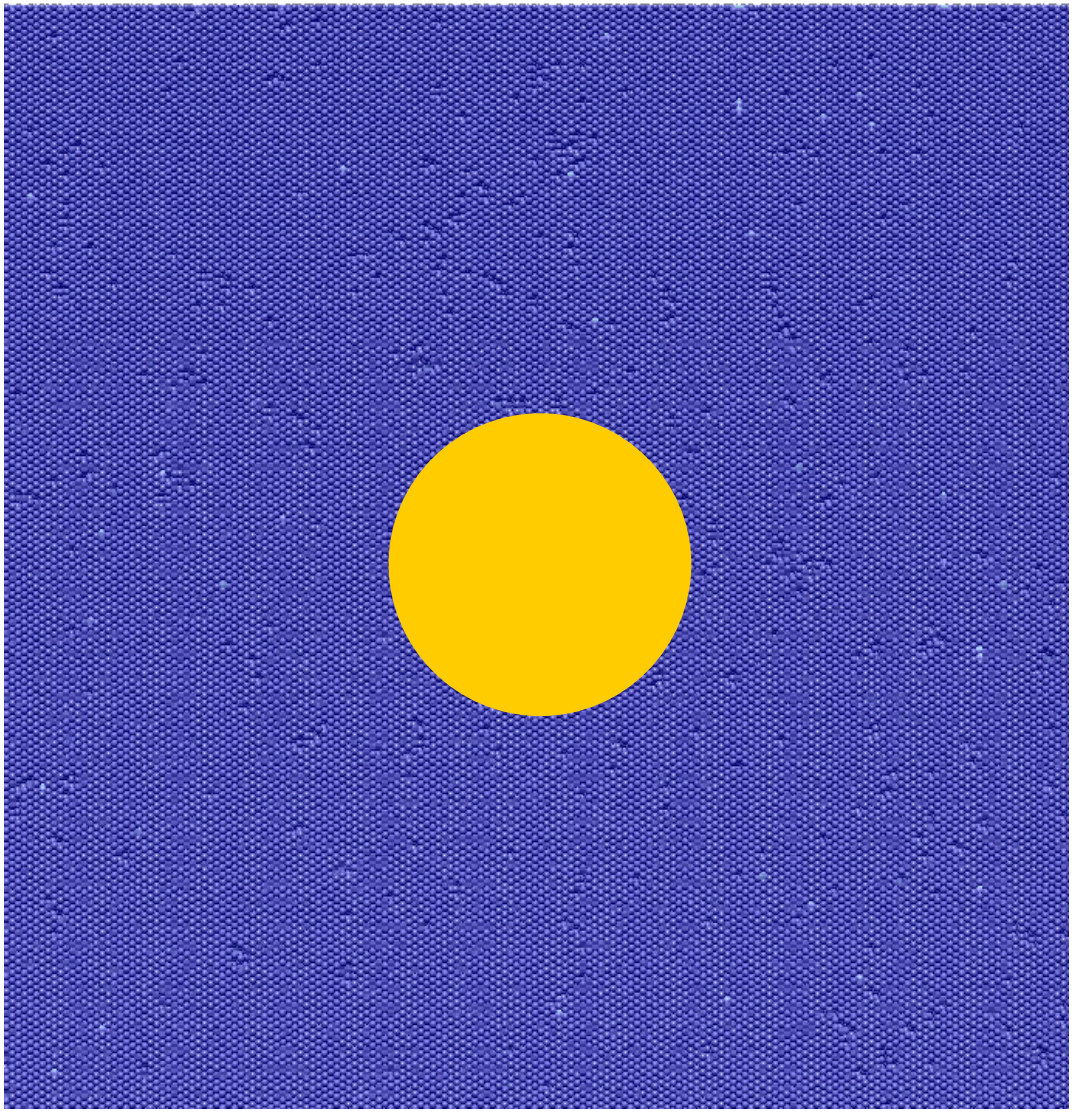

Phases Development in the Range of Swift Ion track

Ni - 40%Al

N = 1 400 000

T = 300 K

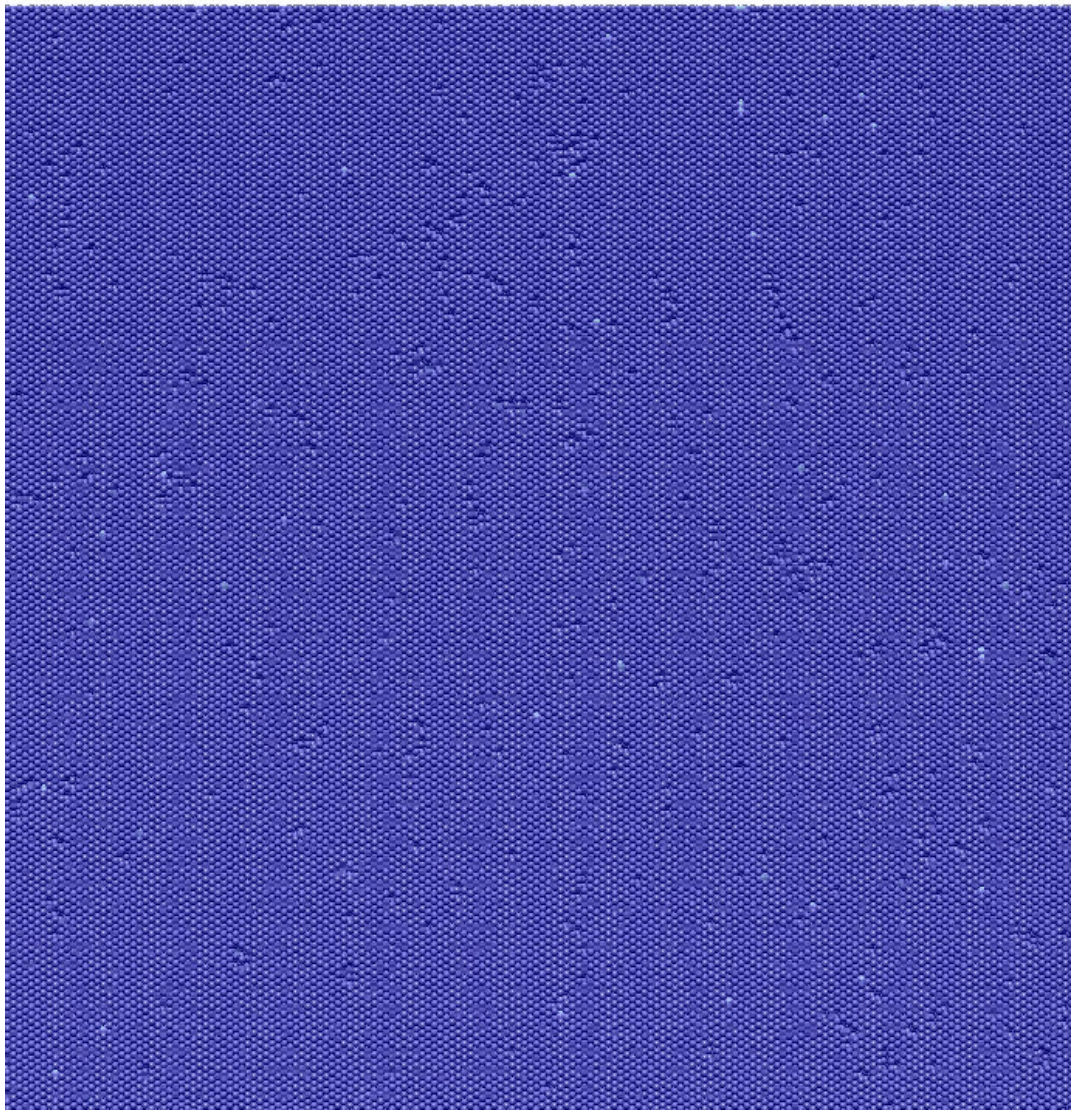

Perfect FCC + HCP
Distorted FCC + HCP
Perfect BCC
Distorted BCC
Perf. & Dist. ICO
Compositionally Disordered
Unclassified

Melting, Martensitic Transformations, Order-Disorder

Simulation setup B

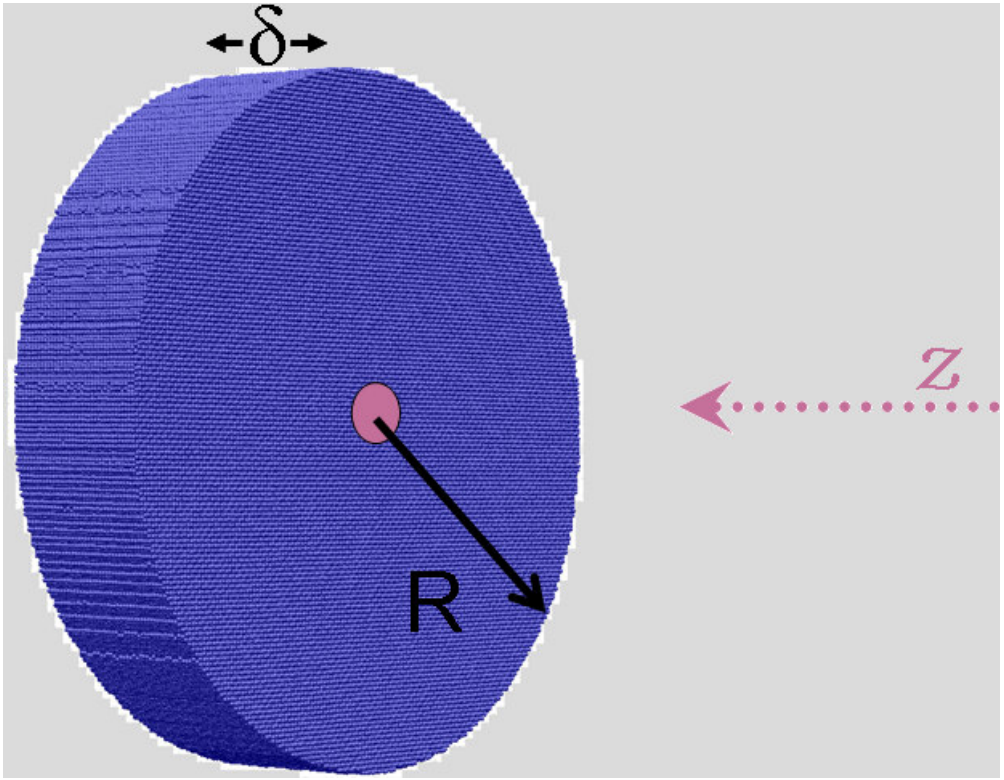

Ni_7Al_5

$\delta = 10\ nm$

R = 22-44 nm

$N = (1\text{-}5) \cdot 10^6$

T = 300-400 K

Development of Swift Ion Track

Ni_7Al_5

N = 1 200 000

T = 300 K

$k_e = 10\ A^2/fs$

8fs
1300K

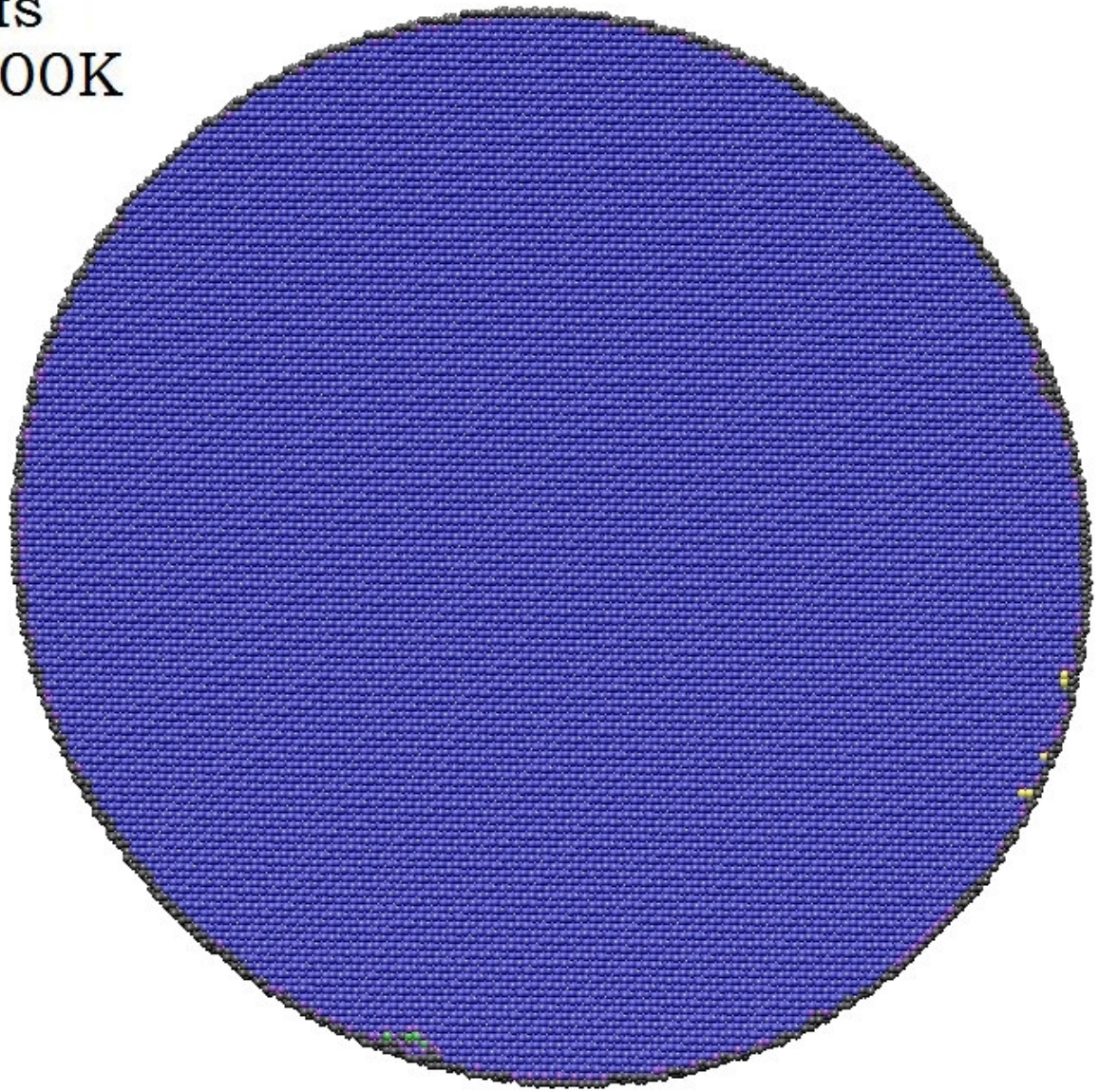

Perfect FCC + HCP
Distorted FCC + HCP
Perfect BCC
Distorted BCC
Perf. & Dist. ICO
Compositionally Disordered
Unclassified

Development of Swift Ion Track

Ni_7Al_5

N = 1 200 000

T = 300 K

$k_e = 5$ A^2/*fs*

8fs
1400K

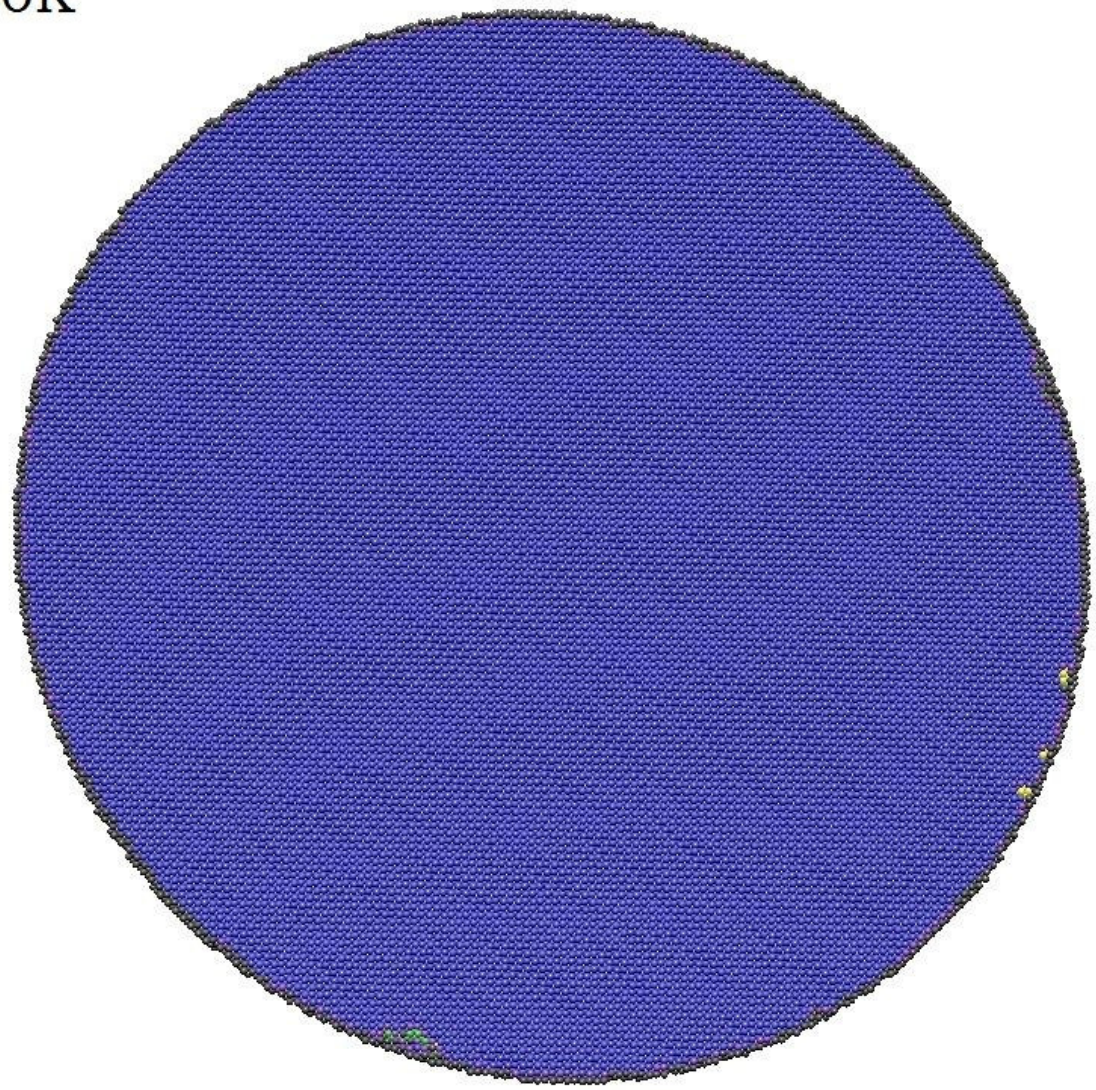

Perfect FCC + HCP
Distorted FCC + HCP
Perfect BCC
Distorted BCC
Perf. & Dist. ICO
Compositionally Disordered
Unclassified

Development of Swift Ion Track

Ni_7Al_5

$N = 4\ 900\ 000$

$T_0 = 400\ K$

$k_e = 10\ A^2/fs$

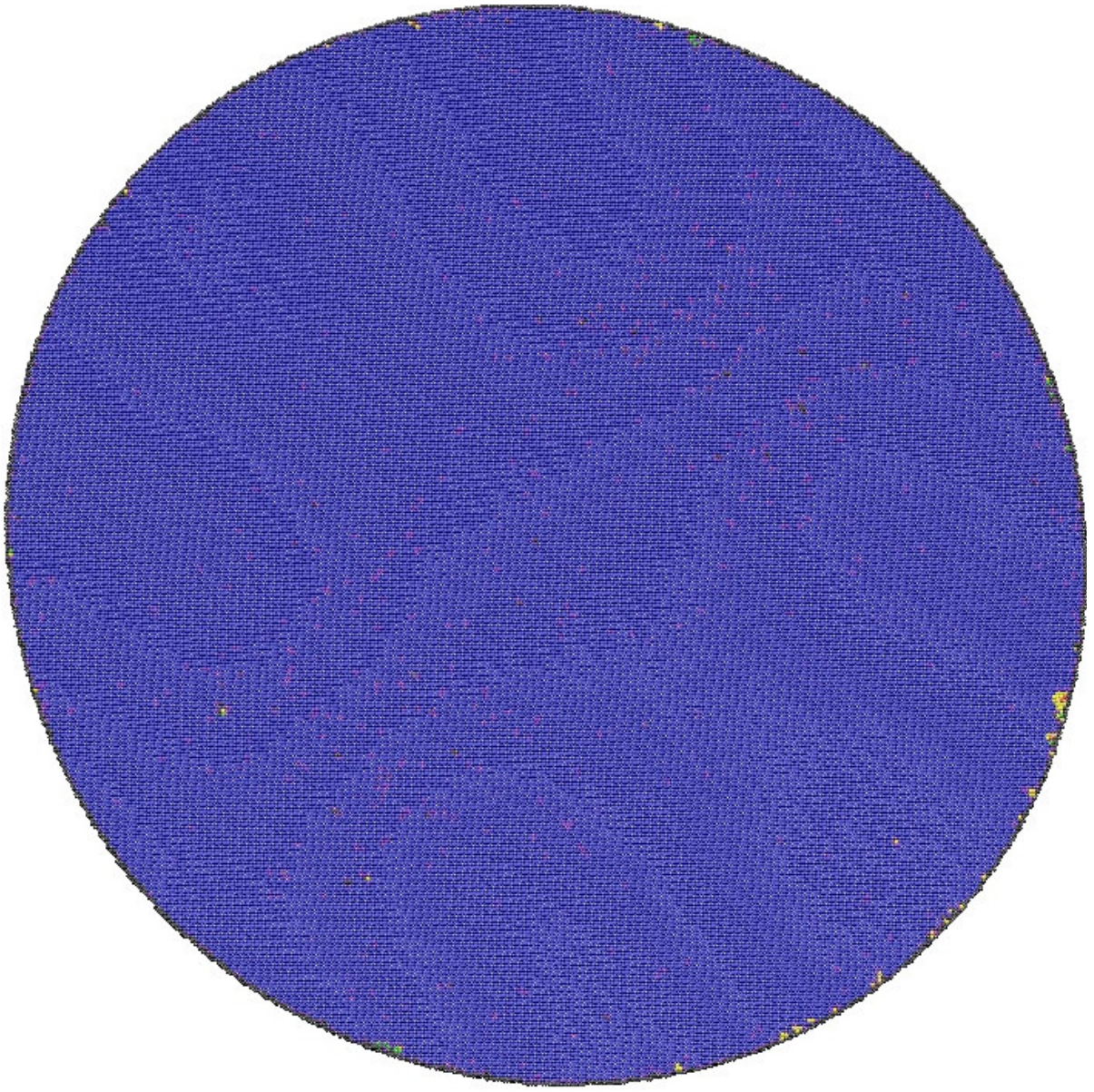

Perfect FCC + HCP
Distorted FCC + HCP
Perfect BCC
Distorted BCC
Perf. & Dist. ICO
Compositionally Disordered
Unclassified

Compositional disordering favours austenitic phase

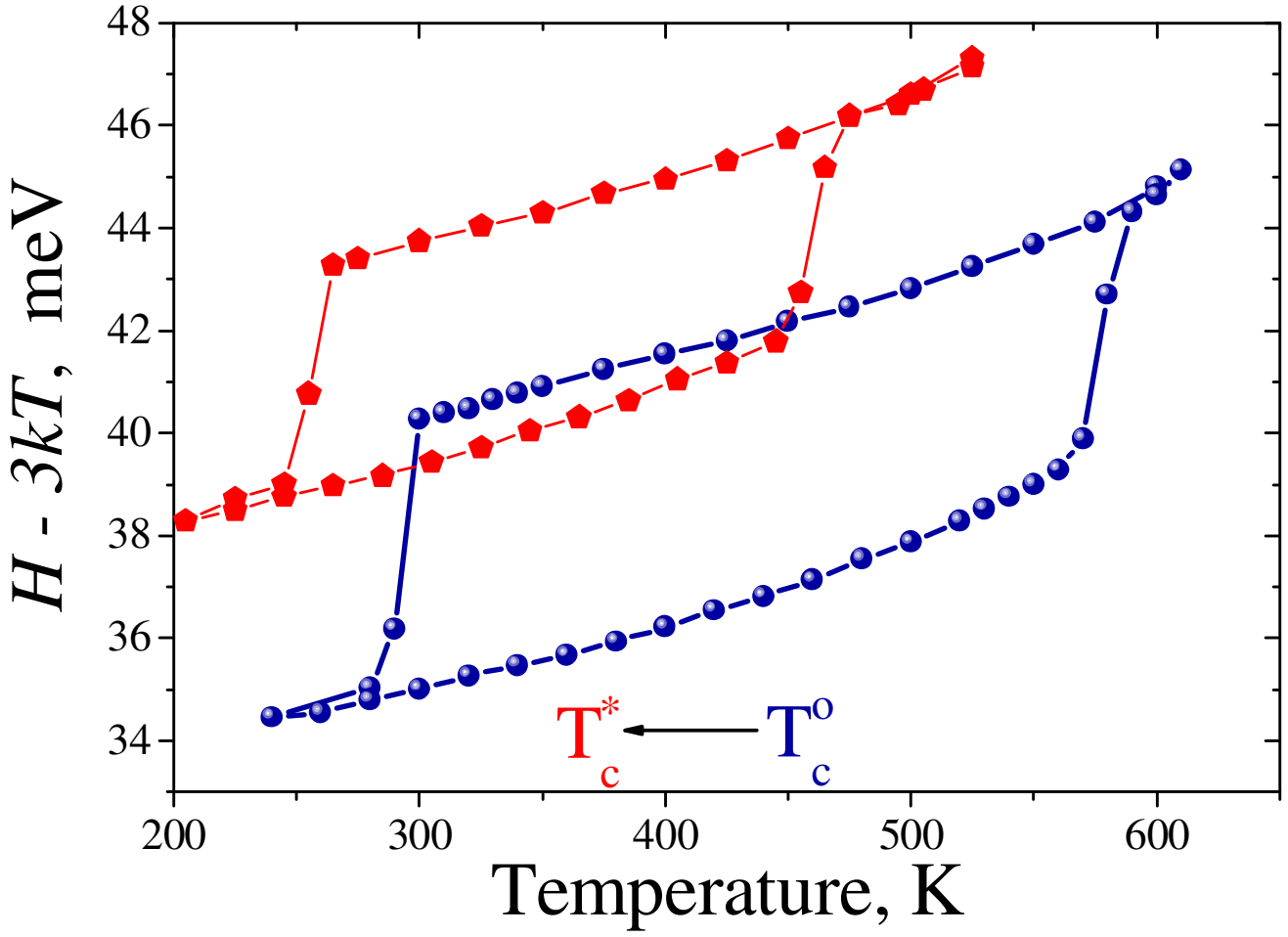

- *Shift of T_c*

Conclusions

- The reversibility of both temperature- and stress-controlled MTs was observed at MD simulation of model NiAl alloy
- Stress-controlled MPTs have features of shape memory effect
- External surface and GG affect the behavior of MTs indicating heterogeneous nucleation of new phase on extended defects
- Compositional disordering is the dominant cause of track formation in ordered NiAl alloy